Age-Related Plasticity in the Synaptic Ultrastructure of Neurons in the Mushroom Body Calyx of the Adult Honeybee *Apis mellifera*

Claudia Groh,[1,2]* Zhiyuan Lu,[2] Ian A. Meinertzhagen,[2] and Wolfgang Rössler[2]

[1]Department of Behavioral Physiology and Sociobiology, Biozentrum, University of Würzburg, Würzburg, 97074, Germany
[2]Department of Psychology and Neuroscience, Life Sciences Centre, Dalhousie University, Halifax, Nova Scotia, Canada B3H 4R2

ABSTRACT

The mushroom bodies are high-order sensory integration centers in the insect brain. In the honeybee, their main sensory input regions are large, doubled calyces with modality-specific, distinct sensory neuropil regions. We investigated adult structural plasticity of input synapses in the microglomeruli of the olfactory lip and visual collar. Synapsin-immunolabeled whole-mount brains reveal that during the natural transition from nursing to foraging, a significant volume increase in the calycal subdivisions is accompanied by a decreased packing density of boutons from input projection neurons. To investigate the associated ultrastructural changes at pre- and postsynaptic sites of individual microglomeruli, we employed serial-section electron microscopy. In general, the membrane surface area of olfactory and visual projection neuron boutons increased significantly between 1-day-old bees and foragers. Both types of boutons formed ribbon and non-ribbon synapses. The percentage of ribbon synapses per bouton was significantly increased in the forager. At each presynaptic site the numbers of postsynaptic partners—mostly Kenyon cell dendrites—likewise increased. Ribbon as well as non-ribbon synapses formed mainly dyads in the 1-day-old bee, and triads in the forager. In the visual collar, outgrowing Kenyon cell dendrites form about 140 contacts upon a projection neuron bouton in the forager compared with only about 95 in the 1-day-old bee, resulting in an increased divergence ratio between the two stages. This difference suggests that synaptic changes in calycal microcircuits of the mushroom body during periods of altered sensory activity and experience promote behavioral plasticity underlying polyethism and social organization in honeybee colonies. J. Comp. Neurol. 520:3509–3527, 2012.

INDEXING TERMS: microglomerulus; projection neuron; Kenyon cell; serial electron microscopy; synaptic plasticity; olfactory

Age- and experience-related neuronal modifications represent important processes underlying behavioral development in a wide range of animal species (for reviews, see Bailey and Kandel, 1993; Kolb and Wishaw, 1998). In insects, for example, various neuropils express age- and experience-related volumetric changes indicating that structural changes in the brain occur that can be related to behavioral plasticity (for reviews, see Meinertzhagen, 2001; Fahrbach, 2006). In the life of a worker honeybee *Apis mellifera*, the transition from nursing inside the hive to outside foraging is accompanied by volume changes in the brain, most notably in the mushroom bodies (Withers et al., 1993; Durst et al., 1994; Fahrbach et al., 1998; Ismail et al., 2006). Despite the clarity of their overall volumetric outcome, we still have little information on the cellular, subcellular, or molecular processes underlying this form of structural plasticity in the course of behavioral maturation (Farris et al., 2001; Seid et al., 2005; Seid and Wehner, 2008; Pasch et al., 2011).

It is now clearly established that the mushroom bodies of insect brains undertake high-level sensory integration and the organization of complex behaviors that involve learning, the formation of associative memories, and

Grant sponsor: Human Frontier Science Program; Grant number: RGP0042/2007-C; Grant sponsor: Deutsche Forschungsgemeinschaft; Grant number: SPP 1392 (to W.R.); Grant sponsor: Natural Sciences and Engineering Research Council; Grant number: DIS-0000065 (to I.A.M.).

*CORRESPONDENCE TO: Claudia Groh, Department of Behavioral Physiology and Sociobiology, Biozentrum, University of Würzburg, Am Hubland, 97074 Würzburg, Germany.
E-mail: claudia.groh@biozentrum.uni-wuerzburg.de

Received January 12, 2012; Revised March 6, 2012; Accepted March 15, 2012
DOI 10.1002/cne.23102
Published online March 20, 2012 in Wiley Online Library (wileyonlinelibrary.com)

orientation (Menzel and Giurfa, 2001; Heisenberg, 2003; Gerber et al., 2004; Davis, 2005; Giurfa, 2007). Synaptic plasticity is a powerful underlying candidate mechanism in the mushroom body's involvement in these behaviors, and is anticipated to underlie adaptations to environmental changes as well as internal changes when the insect undertakes individual tasks (e.g. Technau, 1984; Withers et al., 1993; Gronenberg et al., 1996).

In hymenopteran insects, in particular in ants (Gronenberg et al., 1996; Kühn-Bühlmann and Wehner, 2006; Stieb et al., 2010), bees (Mobbs, 1982; Rybak and Menzel, 1993; Farris et al., 1999; Gronenberg, 2001; Strausfeld, 2002; Groh et al., 2004, 2006; Groh and Rössler, 2011), and social wasps (Ehmer et al., 2001; O'Donnel et al., 2004), the mushroom bodies are particularly large and relative to other brain regions contain large numbers of neurons (Rössler and Groh, 2012). Their main input regions, the calyces, form paired neuropils in each brain hemisphere, each neuropil in turn comprising three anatomically distinct sensory input regions: lip, collar, and basal ring (Fig. 1). The lip receives olfactory information from the ipsilateral antennal lobe and can be further subdivided into a cortical and central input zone innervated by projection neurons from the medial (m) and the lateral (l) antennal-lobe protocerebral tract (APT) (Abel et al., 2001; Kirschner et al., 2006; Zube et al., 2008; Zube and Rössler, 2008; tract nomenclature after Galizia and Rössler, 2010). The collar receives visual information from the ipsi- and contralateral optic lobe via the anterior–superior optic tract, the anterior–inferior optic tract, and the lobular tract (Ehmer and Gronenberg, 2002). Recent studies in bees have revealed that the visual collar is subdivided into layers that are innervated by visual projection neurons transferring chromatic, temporal, and motion-sensitive input from the optic lobe lobula and medulla neuropils (Paulk et al., 2008).

First described from electron microscopy (EM) by Trujillo-Cenóz and Melamed (1962) and Steiger (1967), neuronal circuits within all calycal subregions are organized into an array of synaptic complexes termed microglomeruli. Each microglomerulus consists of a single central presynaptic bouton from the axon terminal of a projection neuron surrounded by numerous postsynaptic profiles, mostly dendritic spines of mushroom body intrinsic neurons called Kenyon cells (Ganeshina and Menzel, 2001; Yasuyama et al., 2002; Frambach et al., 2004; Groh et al., 2004, 2006; Krofczik et al., 2008; Seid and Wehner, 2008; Leiss et al., 2009, Stieb et al., 2010). γ-Aminobutyric acid (GABA)-immunoreactive neurons originating from the mushroom body's output lobes (Grünewald, 1999; Ganeshina and Menzel, 2001; Yasuyama et al., 2002; Leiss et al., 2009) and putative modulatory input from octopamine- and dopamine-positive neurons (Hammer, 1993; Blenau et al., 1999; Hoyer et al., 2005; Sinakevitch and Strausfeld, 2006) together may also contribute to the organization of the microglomeruli. F-actin phalloidin labeling in various insect species, in combination with immunolabeling with an antibody against the highly conserved epitope of a *Drosophila* synaptic vesicle–associated protein, synapsin, demonstrates that Kenyon cell dendritic tips within microglomeruli are highly enriched in F-actin, supporting their spine-like nature (Groh and Rössler, 2011).

The fact that F-actin is concentrated in dendritic spines of Kenyon cells has given rise to the idea that microglomeruli could be sites of structural synaptic plasticity and may play important roles in long-term memory formation. In fact, recent studies in Hymenoptera have shown that the number of adult microglomeruli is affected by brood care (Groh et al., 2004, 2006), sensory experience (Stieb et al., 2010, 2012), and the formation of stable long-term memory (Hourcade et al., 2010).

To gain an understanding of how the mushroom body integrates and stores sensory information from the environment requires first a detailed knowledge of the connectivity and synaptic properties of the circuits in its microglomeruli. In this study we have used electron microscopy to characterize pre- and postsynaptic sites of microglomeruli in the honeybee in order to elucidate how the types and numbers of synapses are adjusted during age-related changes in behavioral development and task performance. We focused on two major unresolved questions: 1) How does the volumetric change in the calyx that occurs during the transition from nursing to foraging depend on the density and total number of calycal presynaptic boutons? and 2) What associated structural changes occur within individual projection neuron boutons and their synapses? Our findings reveal important insights into the plasticity of neural circuits that accompany age-related changes in olfactory and visual processing in the honeybee.

MATERIALS AND METHODS

Animals and cohort experiment

Worker honeybees (*Apis mellifera carnica*) were obtained from a single colony headed by a single-mated queen reared at the institutional apiary at the Biocenter, University of Würzburg, Germany. A cohort experiment was carried out to obtain age-controlled bees. To synchronize the brood, the egg-laying queen was confined to an empty brood comb for 24 hours with a wire-mesh cage that permitted only the passage of workers. At a late pupal stage, the brood comb was transferred to an incubator (Sanyo MIR-153, Bad Nenndorf, Germany), and reared at a constant temperature of 34.5°C. Directly after

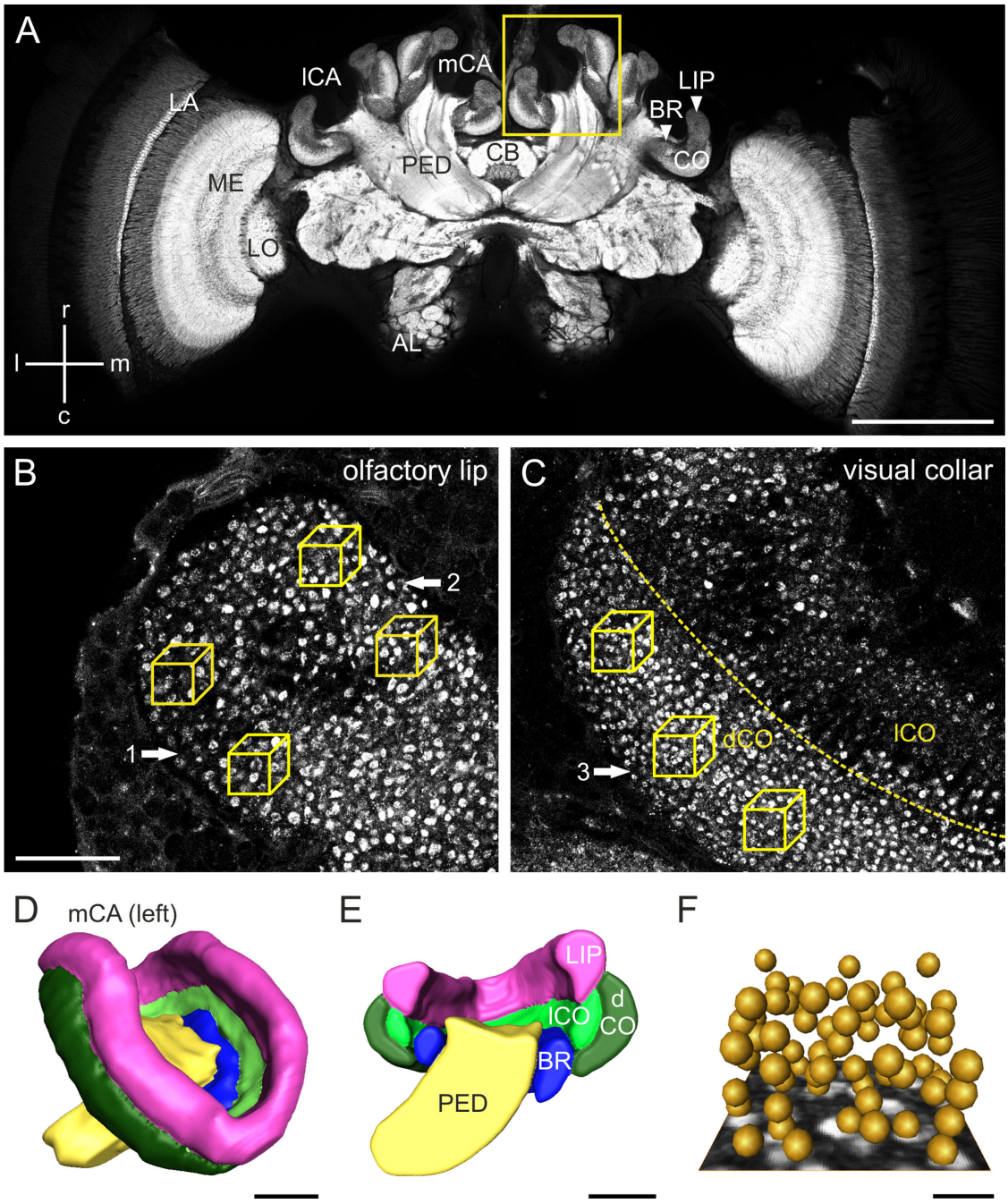

Figure 1. Synapsin immunolabeling and 3D images of the brain of a 35-day-old forager honeybee, *Apis mellifera*. **A:** Single frontal confocal section through a central region of an adult brain viewed as if from the bee's frons, with neuropils immunolabeled for synapsin. Calyx volume and synapsin-labeled bouton density were quantified in the medial calyx (mCA) of the left brain hemisphere (yellow square). Axes (according to Kirschner et al., 2006): caudal (c), lateral (l), medial (m), and rostral (r) apply to the bee's right brain. **B,C:** Enlarged view of the innermost part of the left mCA with synapsin-labeled projection neuron boutons in the lip (B) and the collar (C). Volumes 1–3 (1, m-APT innervated lip; 2, l-APT innervated lip; 3, dense collar) are three regions of interest used to quantify synapsin-labeled boutons. **D,E:** Frontal views of volume reconstruction of the left mCA rendered from confocal image stacks. Entire mCA (D) and cut in a sagittal plane (E) to reveal the lip (magenta), loose collar (lCO; bright green), dense collar (dCO; dark green), and basal ring (BR; blue). As an orientation marker, the mushroom body peduncle (PED; yellow) is also partly reconstructed. **F:** Projection neuron boutons visualized as spheres (yellow) marking the position of each projection neuron center in a 1,000 μm^3 tissue cube (shown for the dense collar) with the original confocal affiliation of a single confocal image. AL, antennal lobe; CB, central body; CO, collar; LA, lamina; lCA, lateral calyx; LO, lobula; ME, medulla. Scale bar = 500 μm in A; 25 μm in B (also applies to C); 100 μm in D (also applies to E); 2 μm in F.

TABLE 1.
Primary Antibody Used in This Study

Antibody	Immunogen	Manufacturer
Synapsin	*Drosophila* synapsin protein fused to glutathione-S-transferase, protein accession #CAA64723	DSHB (Iowa City, IA), 3C11 (anti SYNORF1) mouse (monoclonal)

emergence, 1-day-old (≤24 hours old) honeybees (~500) were collected from the brood comb. The bees were either immediately processed for immunohistochemical procedures (referred to as 1-day-old bees) or marked with a white spot on the dorsal surface of the thorax, and transferred back into the natal colony. Marked bees were collected as pollen foragers at the age of 35 days after returning from a foraging trip carrying pollen loads on their legs (referred to as 35-day-old pollen foragers).

Antibody characterization

For synapsin immunolabeling, we used a monoclonal mouse antibody against the *Drosophila* synaptic vesicle–associated protein synapsin I (SYNORF1; Table 1; kindly provided by E. Buchner, University of Würzburg, Germany). SYNORF1 was raised against a 66-kDa 3′-fusion protein comprising a synapsin protein 5′ fragment corresponding to the nucleotide sequence 621–1967 fused to glutathione-S-transferase (Klagges et al., 1996). In western blots of brain homogenates, the antibody detects in *Drosophila* several prominent bands (a protein triplet of 70, 74, and 80 kDa and a protein doublet at 143 kDa; Klagges et al., 1996) and in *Apis* a protein doublet at 72 kDa (Pasch et al., 2011). All these different bands are believed to originate from different synapsin isoforms (Klagges et al., 1996), and the exact recognized epitope (amino acids 341 LFGGMEVCGL 350) has been reported (Hofbauer et al., 2009). The specificity of SYNORF1 has been confirmed in a null mutant of *Drosophila*, *syn*^{79}, which lacks expression of any of the wild-type synapsin isoforms at 70–80 kDa and 143 kDa in both western blots and after immunohistochemistry (Godenschwege et al., 2004). In a recent study, the same antibody was shown to label presynaptic terminals in a similar pattern in the honeybee (Pasch et al., 2011) and across a wide range of neopteran insects (Groh and Rössler, 2011). Alexa Fluor 488–conjugated goat anti-mouse secondary antibody (A-11001, Molecular Probes, Eugene, OR) was used to detect mouse anti-synapsin.

Neuroanatomical procedures

Synapsin immunolabeling of whole-mount preparations

To analyze age-related influences on structural plasticity of calycal microglomeruli, we established a protocol to immunolabel presynaptic terminals in whole-mount preparations. One- and 35-day-old worker bees were anesthetized with CO_2, and the heads were fixed with dental wax (Surgident, Sigma Dental Systems, Handewitt, Germany) in customized acrylic blocks. The heads were entirely covered with cold physiological saline (130 mM NaCl, 5 mM KCl, 4 mM $MgCl_2$, 5 mM $CaCl_2$, 15 mM Hepes, 25 mM glucose, 160 mM sucrose; pH 7.2). A window was cut frontally into the head capsule, glands and tracheae were removed, and the proboscis was dissected off. Animals were decapitated and the heads were immediately immersed overnight in ice-cold 4% formaldehyde (FA; methanol free, 28908, Fischer Scientific, Schwerte, Germany) in 0.01 M phosphate-buffered saline (PBS; pH 7.2) at 4°C. The fixed brains were dissected out under PBS, and the retinae and ocelli were removed.

After washes in PBS (5X 10 minutes), brains were permeabilized in 0.2% Triton X-100 (Tx) in PBS (2X 10 minutes), and then blocked in 2% normal goat serum (NGS; 005-000-121, Jackson ImmunoResearch Laboratories, West Grove, PA) in 0.2% PBS-Tx for 1 hour at 23°C. For synapsin immunohistochemistry, brains were incubated in the primary antibody SYNORF1, diluted 1:10 in 0.2% PBS-Tx with 2% NGS for at least four nights at 4°C. After rinses in PBS (5X 10 minutes), brains were incubated in Alexa Fluor 488–conjugated goat anti-mouse secondary antibody (1:250) in 1% NGS-PBS for four nights at 4°C. Brains were then washed in PBS (5X 10 minutes) and dehydrated in an ascending ethanol series (30%, 50%, 70%, 90%, 95%, 3X 100%, 10 minutes per step). Finally, all brains were cleared and mounted in methyl salicylate (M-2047, Sigma Aldrich, Steinheim, Germany) by using custom aluminum slides with a central hole covered from both sides by #00 coverslips (55–80 μm thick, 5812914, Fisher Scientific).

Tissue preparation for conventional EM and serial sectioning

For serial-section electron microscopy (ssEM), 1- and 35-day-old bees were immobilized with CO_2 and decapitated. Their heads were fixed in dental-wax–coated dishes, and covered with cold physiological saline. After dissection, brains were immediately transferred into modified Karnovsky's fixative overnight at 4°C, as previously reported (Meinertzhagen, 1996). Brains were washed in 0.1 M cacodylate and 0.04% $CaCl_2$ (3X 15 minutes), embedded in 5% low melting point agarose

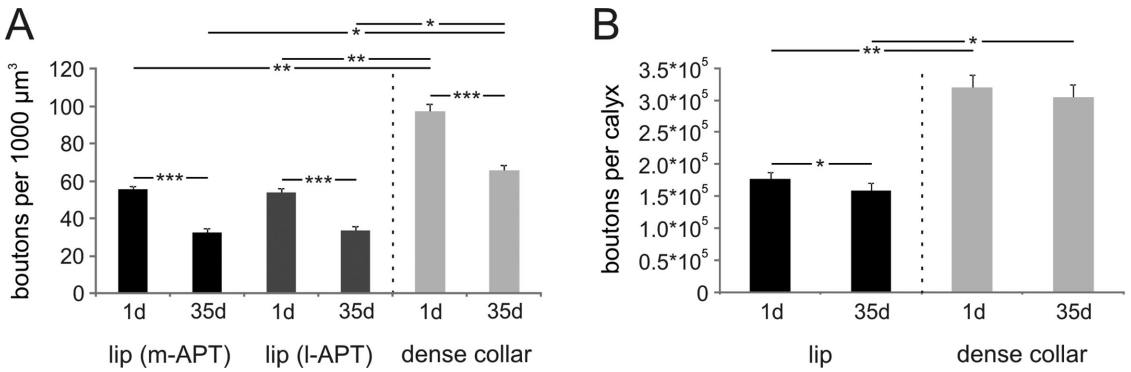

Figure 2. Changes in the numbers of synapsin-labeled boutons in the calyx counted in whole-mount preparations of 1- and 35-day-old worker bees. **A:** Age-related decrease in the packing density of synapsin-labeled boutons within 1,000 µm^3 of neuropil in the medial antennal-lobe protocerebral tract (m-APT) and the lateral (l)-APT innervated lip and the dense region of the collar. **B:** Estimated total number of synapsin-labeled boutons in the lip and dense collar of the left medial calyx.

(Agarose II, no. 210-815, Amresco, Solon, OH), and sectioned at 150 µm in a horizontal plane on a vibrating blade microtome (Leica VT 1000S, Nussloch, Germany). After the agarose was removed, brain slices were post-fixed in 2% aqueous OsO_4 (Roth, Karlsruhe, Germany) buffered with 0.3 M cacodylate for 2 hours at 23°C. They were then washed in 50% ethanol for several seconds, before further dehydration in a graded ethanol series (50%, 70%, 90%, 95%, 2X 100%, 10 minutes per step) followed by propylene oxide (2X 10 minutes). The tissues were infiltrated overnight in a 1:1 mixture of propylene oxide and Poly/Bed812 (Electron Microscopy Sciences, Munich, Germany) at 23°C, before being transferred from the mixture into pure Poly/Bed 812 for 4 hours at 23°C. For final embedding, brain slices were placed in disposable aluminum weighing dishes filled with fresh Poly/Bed 812 and polymerized for 48 hours at 60°C.

The resulting resin blocks were manually trimmed with a razor blade under a dissecting microscope to the region of interest (left medial calyx and central complex). Semithin 1–2 µm sections were cut in a horizontal plane with a microtome (Reichert Jung 2050). Only the innermost part of the left medial calyx was cut in ultrathin series. About 200 serial ultrathin sections were then cut at 50 nm, collected on Pioloform-coated 1 × 2 mm slot grids, and stained first with saturated aqueous uranyl acetate for 10 minutes and then with lead citrate for 5 minutes.

Microscopy, image processing, and data acquisition

Laser-scanning confocal microscopy, image processing, and data acquisition

Whole mount preparations of 1-day-old ($n = 11$) and 35-day-old bees ($n = 7$) were scanned by using a laser-scanning confocal microscope (Leica TCS SP2, Leica Microsystems, Wetzlar, Germany) equipped with an argon/krypton laser. Optical sections were taken at a resolution of 1,024 × 1,024 pixels. For volume measurements of synapsin-immunolabeled calycal subregions, optical sections through the entire left medial calyx (box in Fig. 1A) were taken at 5 µm intervals (10×/0.4 NA imm; digital zoom 3.0–3.5). To investigate plastic changes in the density of synapsin-positive boutons in the lip and dense region of the collar, the innermost part of the left medial calyx was scanned at high resolution through a depth of 10 µm at intervals of 0.5 µm (63×/1.4 NA imm; digital zoom 2).

Digital image stacks were further processed by using 3D software (AMIRA 5.3; Mercury Computer Systems, Berlin, Germany). For volume measurements of calycal subregions, the neuropil boundaries of the lip, collar (the separate dense and loose regions), and basal ring were traced manually on each section by using the AMIRA segmentation editor, as previously reported (Brandt et al., 2005). Traced profiles were stored in separate image volumes, and the label fields were used for conventional volumetric analysis (Fig. 1D,E). To quantify synapsin-positive boutons, labeled puncta were counted in defined volumes each of 1,000 µm^3 in three regions of interest by using the AMIRA landmark viewer (Fig. 1B,C). These were: two volumes per m-APT and l-APT innervated lip region, respectively, and three volumes per dense collar. Digital filters were applied to sharpen faint contours of synapsin-labeled boutons, and bouton-size adjusted landmarks were used to facilitate counting boutons in consecutive sections (Fig. 1F). Only boutons with outlines falling mostly within those volumes were included in the counts. All counts were done blind, without knowledge of the age group. In the lip and the dense collar, bouton numbers were averaged separately for each individual, and a mean

of the means was calculated based on the number of brains investigated per group (Fig. 2). To estimate the total bouton number per calyx lip and per dense collar, mean bouton numbers per 1,000 μm^3 were extrapolated to the volume of the respective subregion of the calyx.

Electron microscopy, image processing, and data acquisition

Serial ultrathin sections were examined at 80 kV in a Philips Tecnai 12 EM (Fig. 3). Digital images from three regions of interest (white boxes in Fig. 3A) were captured from ~200 serial sections from a 1-day-old and a 35-day-old bee. A complete stack in each region of interest covered a volume of about 4,320 μm^3 (24 $\times$ 18 $\times$ 10 μm) for the 1-day-old bee and 5,200 μm^3 (26 $\times$ 20 $\times$ 10 μm) for the 35-day-old bee. Occasional folds in the sections were corrected, and each section was manually aligned in Adobe Photoshop CS2 (Adobe Systems, San Jose, CA). To make these corrections, areas of tissue that were not visible in their entirety because of a fold in the section were substituted with an insertion of the same area from an adjacent section to permit vertical alignment. Consecutive sections were aligned manually by using sEM Align (Fiala and Harris, 2001). Cell profiles were traced to generate 3D reconstructions by using additional software (Reconstruct; Fiala, 2005).

The shape and size of projection neuron boutons, their synapses, and their postsynaptic partners in the brains of a 1- and 35-day-old bee were quantified. Cell types were identified in ssEM based on previous reports that used immuno-EM to characterize choline acetyltransferase (ChAT)-positive projection neuron boutons, Kenyon cells, and GABA-immunoreactive extrinsic neurons (ENs) of calycal microglomeruli (*Apis*: Ganeshina and Menzel, 2001; *Drosophila*: Yasuyama et al., 2002). In short, axonal boutons of projection neurons are the largest vesicle-packed elements that can be identified in the mushroom body calyx (Fig. 3), and they contain clusters of prominent mitochondria and numerous presynaptic specializations (visible from their electron-dense staining at the cell membrane). The projection neuron boutons are largely presynaptic to numerous tiny, vesicle-free profiles of Kenyon cell dendrites. EN profiles are smaller than and often accessory to projection neurons, exhibiting a sparsely filled cytoplasm marked by occasional presynaptic sites.

Using these criteria, all potential projection neuron bouton profiles in the series were traced manually to generate 3D reconstructions. Projection neuron boutons have previously been shown to differ in their cytoplasmic electron density and are referred to here as light and dark boutons; this difference most likely reflects the density and distribution of small clear-core vesicles in the cytoplasm (Ganeshina and Menzel, 2001). To estimate the vesicle packing densities within each bouton, 8-bit gray scale values (0–255) in circular areas, each having a diameter of 250 nm, as shown in Figure 3C and D, were measured in any given section plane in regions of cytoplasm free of mitochondria and dense-core vesicles by using ImageJ (FIJI based on ImageJ 1.44c, Wayne Rasband, NIH, Bethesda, MD). Then, a mean gray value per bouton was calculated. Boutons with gray scale values $>$ 180 were classified as light boutons, and boutons with gray scale values $\leq$ 180 as dark boutons. To estimate the density of projection neuron boutons within each region of interest, bouton numbers were counted in a normalized volume of 1,000 μm^3.

Synaptic contacts were identified by the presence of pre- and postsynaptic densities between projection neuron boutons and adjacent postsynaptic profiles (mostly Kenyon cell dendrites), and by the electron-dense staining at the presynaptic membrane designating the active zone (Ganeshina and Menzel, 2001; Seid et al., 2005). In 10 projection neuron boutons per region of interest selected from their mean surface areas, each presynaptic specialization was counted as a single active zone; more than one postsynaptic partner was almost always present. Each profile in direct contact with the active zone situated beneath the active zone when viewed in consecutive sections was counted as a single postsynaptic contact. This method thus provided a measure of the total number of postsynaptic partners at the entire active zone, and thus of the synaptic divergence.

Statistical analysis

Mann–Whitney U-tests were used for statistical comparisons of several parameters recorded for projection neuron boutons of the same neuropil region of interest, across the two age groups sampled. Differences between neuropil regions of interest within the same age group were tested by using the Wilcoxon test. Data are presented as mean $\pm$ SD. The Kruskal-Wallis test was used to compare how often particular numbers of profiles occurred postsynaptic to active zones. Box plots give the median and the 25% and 75% quartiles in the box of the observed values. A chi-square test was used to test for age-related changes in the percentages of the two following parameters: percentage of both light and dark boutons per neuropil region of interest; and ribbon and non-ribbon synapses per projection neuron bouton. The α level was set at 0.05 and, when multiple significance tests were performed, the Bonferroni-adjusted α level was set at 0.017 to limit the overall experiment-wise error rate. Statistical analyses were performed with SPSS 15.0 software (SPSS, Chicago, IL). Graphs and figures were edited by using Corel Draw X3 (Corel, Ottawa, Canada) and, in some cases, adjusted for brightness and contrast.

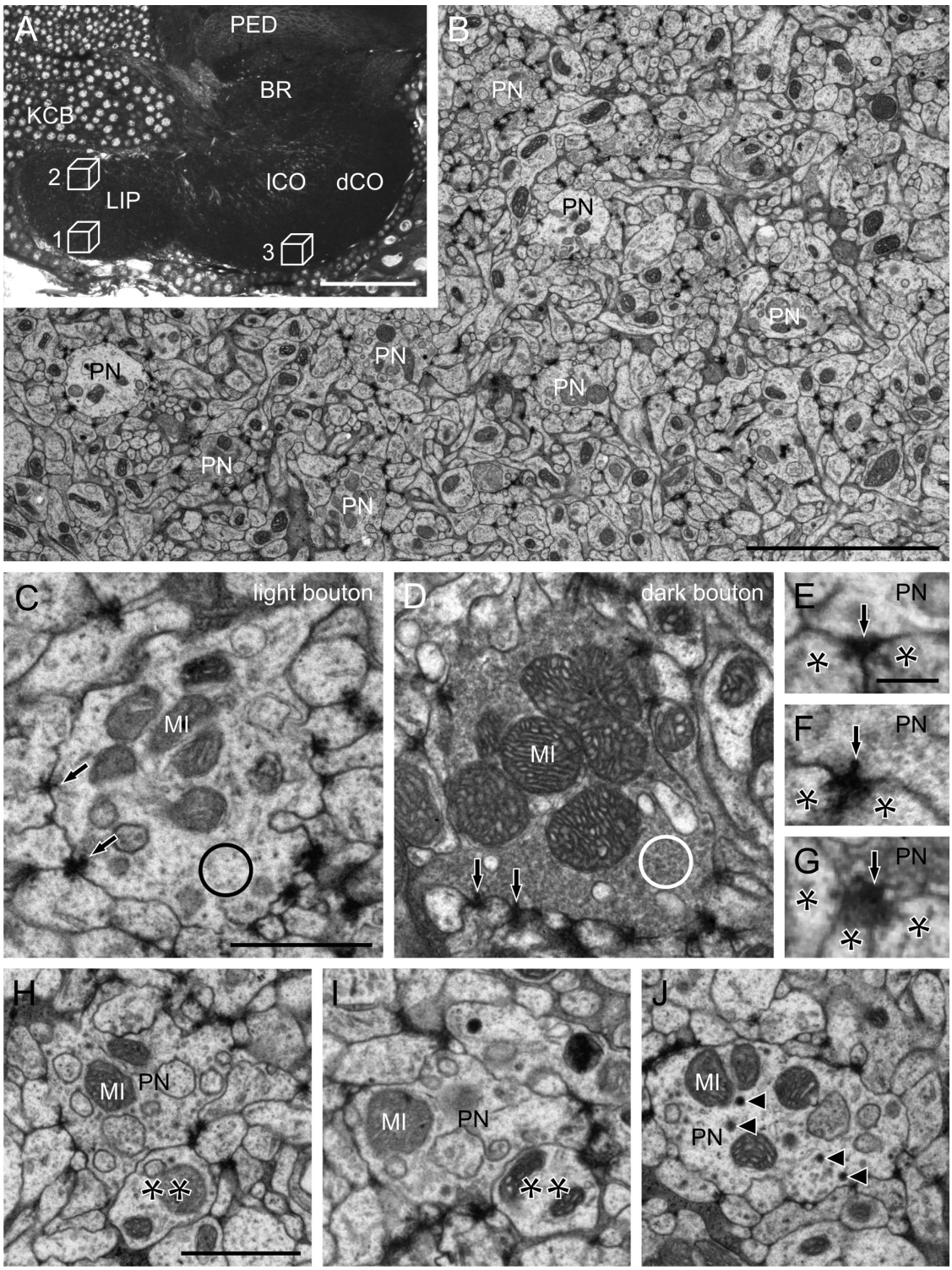

Figure 3. Composition of the honeybee calycal neuropil. **A:** Innermost part of the left medial calyx, frontal semithin section stained with toluidine blue. **B:** Electron micrograph of the dense collar region of the calyx of a 1-day-old bee. Profiles of projection neuron boutons are densely packed. Those that could be reconstructed in their entirety within the series are labeled. **C,D:** Light (C) and dark (D) boutons showing differences in cytoplasmic electron density (quantified from the gray-scale values within circles). **E–G:** Synaptic characteristics of projection neuron boutons. Presynaptic sites are either non-ribbon (E) or ribbon synapses (F,G). Ribbon synapses exhibit either solely a pedestal (F) or have a pedestal with platform (G). Postsynaptic profiles are marked with a single asterisk; arrows at presynaptic sites show the presumed direction of transmission. **H–J:** Extrinsic neurons (asterisks in H,I) are sometimes associated with projection neuron boutons as joint members of a microglomerulus. Boutons only occasionally contain dense-core vesicles (arrowheads in J). BR, basal ring; dCO, dense collar; KCB, Kenyon cell body; ICO, loose collar; MI, mitochondrion; PED, peduncle; PN, projection neuron. Scale bar = 50 μm in A; 5 μm in B; 1 μm in C (also applies to D); 200 nm in E (also applies to F,G); 1 μm in H (also applies to I,J).

TABLE 2.

Volume of Calycal Subcompartments, Numbers of Projection Neuron Boutons, and Their Packing Densities[1]

Neuropil	Age (days)	Volume ($\mu m^3 \times 10^6$)	Volume increase (%)	Bouton per 1,000 μm^3	Bouton per calyx ($\times 10^5$)
Lip	1	3.24 ± 0.12	–	55.50 ± 1.66	1.77 ± 0.10
	35	4.72 ± 0.26	45.68	32.86 ± 1.86	1.58 ± 0.13
Dense collar	1	3.31 ± 0.18	–	97.00 ± 4.06	3.20 ± 0.20
	35	4.64 ± 0.36	40.18	65.90 ± 2.48	3.05 ± 0.19
Loose collar	1	1.42 ± 0.12	–	–	–
	35	1.88 ± 0.17	32.39	–	–
Collar (total)	1	4.73 ± 0.28	–	–	–
	35	6.52 ± 0.48	37.84	–	–
Basal ring	1	1.18 ± 0.09	–	–	–
	35	1.73 ± 0.09	46.61	–	–

[1]3D volume reconstruction of calycal subcompartments and quantification of calycal projection neuron bouton number and density based on synapsin-labeled whole-mount preparations of young and old bees. Calycal subcompartments of the calyx are significantly larger in foragers than in freshly emerged bees. Values are presented as means (± SD) calculated from 11 freshly emerged and 7 forager bees. As projection neuron bouton density did not differ between the m-APT and l-APT, both mean bouton number per 1,000 μm^3 and estimation of total projection neuron bouton number in the lip are based on calculations in the m-APT innervated lip.

RESULTS

Synapsin immunolabeling in whole-mount preparations

In this study we introduced a protocol for synapsin immunolabeling of whole-mount preparations that allowed us to combine volume measurements of the calyx with the quantification of synapsin-positive presynaptic boutons in the calyx of adult honeybees. In general, this technique showed only minor gradients of synapsin-antibody penetration from the surface to the center of the brain. At low magnification, all major neuropils such as the antennal lobes, optic lobes, mushroom bodies, or the central body could be readily identified (Fig. 1A). Deep-lying neuropils such as the central body and the mushroom body stalks were revealed with clarity and the mushroom body subdivisions could be distinguished along the depth of the entire calyx. At high magnification, anti-synapsin labeling revealed distinct synapsin-immunoreactive (IR) boutons in all subregions of the calyx (Fig. 1B,C). Some synapsin-positive bouton profiles lacked signal at their core that was attributed to a central accumulation of mitochondria (Frambach et al., 2004; Leiss et al., 2009). In the collar (Fig. 1C), synapsin-IR boutons were densely packed and homogenously distributed in the outer region (dense collar) and more loosely arranged in the inner region (loose collar). Given their uneven distribution in the loose-collar region, bouton density was only quantified in the dense region of the collar (see below). In aggregate, our observations on synapsin-labeled synaptic boutons in the adult calyx of bee whole-mounts corroborate, but with far greater efficiency, earlier descriptions on the distribution of synapsin immunoreactivity based on brain sections (Groh et al., 2004, 2006; Groh and Rössler, 2011).

Age-related changes in the density of synapsin-IR boutons within calycal subdivisions

The mushroom body calyx lip receives primarily olfactory input via the m- and l-APT, whereas the dense collar receives visual input, and the basal ring receives input from both modalities (Gronenberg, 2001; Ehmer and Gronenberg, 2002; Kirschner et al., 2006). To quantify the density of boutons in the two regions with the clearest separation of sensory input, the lip and the dense collar region, we counted synapsin-labeled boutons in defined tissue blocks in the inner region of the left medial calyx of 1-day- and 35-day-old bees (Fig. 1B,C,F). Synapsin-labeled boutons in the mushroom body calyx were less densely packed in the m- and l-APT innervated lip (Fig. 1B) than in the dense collar region (Fig. 1C). This difference was found both in 1-day-old bees (Fig. 2A and Table 2; Wilcoxon test, Bonferroni corrected: m-APT–dense collar, $P < 0.003$; l-APT–dense collar, $P < 0.003$) and 35-day-old bees (Wilcoxon test, Bonferroni corrected: m-APT–dense collar, $P < 0.017$; l-APT–dense collar, $P < 0.017$). The density of synapsin-labeled boutons between the m- and l-APT innervated lip did not differ significantly in 1-day-old (Wilcoxon test, Bonferroni corrected: m-APT–l-APT: $P > 0.017$) and 35-day-old bees (Wilcoxon test, Bonferroni corrected: m-APT–l-APT, $P > 0.017$). Overall, the packing density of presynaptic boutons decreased significantly by 35–40% in 35-day-old foragers compared with 1-day-old bees in all three regions of interest (Mann–Whitney U-test: m-APT: 1 day–35 days, $P < 0.001$; l-APT: 1 day–35 days, $P < 0.001$; dense collar, $P < 0.001$).

To quantify age-related volume changes, all subregions of the entire left medial mushroom body calyx of 1- and 35-day-old bees were traced manually on each slice by

using the AMIRA segmentation editor, and the 3D reconstructions generated (Fig. 1D,E). The resulting volumes of the various subregions of the calyx were significantly larger in foragers compared with 1-day-old bees (Table 2; Mann–Whitney U-test: lip: 1 day–35 days, $P < 0.001$; dense collar: 1 day–35 days, $P < 0.001$; loose collar: 1 day–35 days: $P < 0.001$; collar total: 1 day–35 days: $P < 0.001$; basal ring: 1 day–35 days: $P < 0.001$). The age-related volume increase we observed from our whole-mount preparations confirms by more direct measures the earlier volumetric studies based on more laborious serial section methods (Durst et al., 1994), whereas the volume dimensions of the calycal subdivisions of foragers are comparable to those found by Brandt et al. (2005) using synapsin-labeled whole-mount preparations.

Does the decreased volumetric density of synapsin-labeled boutons in the lip and dense collar regions simply result from the increased spacing between boutons caused by the observed volume increase (Fig. 2; Withers et al., 1993; Durst et al., 1994; Fahrbach et al., 1998; Ismail et al., 2006), or is there a difference in the total number of boutons? To estimate the total bouton number per calyx lip and per dense collar, the mean bouton numbers per 1,000 μm^3 were extrapolated to the volume of the respective calycal subregion (Fig. 2B and Table 2). We found significantly fewer synapsin-labeled boutons in the lip compared with the dense region of the collar in both 1-day (Wilcoxon test: $P < 0.01$) and 35-day-old bees (Wilcoxon test: $P < 0.05$). In the lip region, a significant decrease in the total number of boutons also occurred in bees between 1 and 35 days of age (Mann–Whitney U-test: $P < 0.05$). In the dense region of the collar, the total number of synapsin-IR boutons did not differ significantly between 1- and 35-day-old bees, however (Mann–Whitney U-test: $P > 0.05$). Altogether, these results indicate that the volume increase of the calyx in foragers is not caused by a simple increase in projection neuron bouton number, rather the opposite is true: there tend to be fewer boutons.

Morphological and ultrastructural features of projection neuron boutons in ssEM

To examine the ultrastructural features of calycal microglomeruli we made 3D reconstructions from serial electron micrographs of projection neuron boutons (Fig. 3B–D) and analyzed the synaptic sites and their postsynaptic profiles; the latter arose from Kenyon cells (Fig. 3E–G) and extrinsic neuron terminals (Fig. 3H–J). The boutons were identified by their size (larger than all the other elements in serial sections), and by the close spacing of active zones, as previously reported in *Apis* (Ganeshina and Menzel, 2001), *Drosophila* (Yasuyama et al., 2002; Leiss et al., 2009; Butcher et al., 2012) and in ants (Seid et al., 2005; Seid and Wehner, 2008, 2009). The synaptic boutons formed by projection neurons were the most prominent features of the calycal region, containing numerous (6 ± 2) entire mitochondria clustered in the center (Fig. 3B–D).

Three-dimensional reconstructions revealed morphologically distinct types of terminal boutons (Fig. 4). Those in the m-APT and l-APT innervated lip region were polymorphic, classified as unilobed (with a single round bouton), clustered (with multiple round terminals in close proximity, together forming a large bouton complex), or elongated (Fig. 4A). Visual projection neuron boutons in the dense region of the collar were by contrast usually unilobed (Fig. 4B). Long, slender axons were visible in some reconstructions, but for technical reasons only short segments could be reconstructed in others. The axons themselves did not form presynaptic sites; instead the projection neuron boutons always formed at axon terminals.

Boutons in the m-APT and l-APT innervated lip region differed significantly in their surface areas, being on average about twice as large as boutons in the dense collar region in both 1-day-old (Fig. 5A; Wilcoxon test, Bonferroni corrected: m-APT–dense collar, $P < 0.0003$; l-APT–dense collar, $P < 0.0003$) and 35-day-old bees (Wilcoxon test, Bonferroni corrected: m-APT–dense collar, $P < 0.0003$; l-APT–dense collar, $P < 0.0003$).

We also found an age-related difference in the surface area between projection neuron boutons in the m- and l-ATP innervated lip region. In the 1-day-old bee, we found no significant difference in bouton surface area between the two regions (Wilcoxon test, Bonferroni corrected: m-APT–l-APT,: $P > 0.017$), whereas boutons in the l-APT innervated lip region of the 35-day-old bee were significantly larger than those in the m-APT innervated lip (Wilcoxon test, Bonferroni corrected, $P < 0.003$). Both olfactory and visual boutons showed a significant age-related increase in surface area between the 1-day-old and forager bees (Mann–Whitney U-test: m-APT: 1 day–35 days, $P < 0.01$; l-APT: 1 day–35 days, $P < 0.001$; dense collar: 1 day–35 days, $P < 0.001$). Similarly, boutons both in the m-APT and l-APT innervated lip region were significantly larger in volume than boutons in the dense collar region in a 1-day-old (Fig. 5B; Wilcoxon test, Bonferroni corrected: m-APT–dense collar, $P < 0.0003$; l-APT–dense collar, $P < 0.0003$) and a 35-day-old bee (Wilcoxon test, Bonferroni corrected: m-APT–dense collar, $P < 0.0003$; l-APT–dense collar, $P < 0.0003$).

Bouton volumes in the m-APT and l-APT showed no significant differences at day 1 (Wilcoxon test, Bonferroni corrected: m-APT–l-APT, $P > 0.017$), but boutons in the l-APT innervated lip region of the 35-day-old bee were significantly larger than those in the m-APT innervated lip (Wilcoxon test, Bonferroni corrected, $P < 0.0003$). Olfactory and visual boutons were both significantly larger in

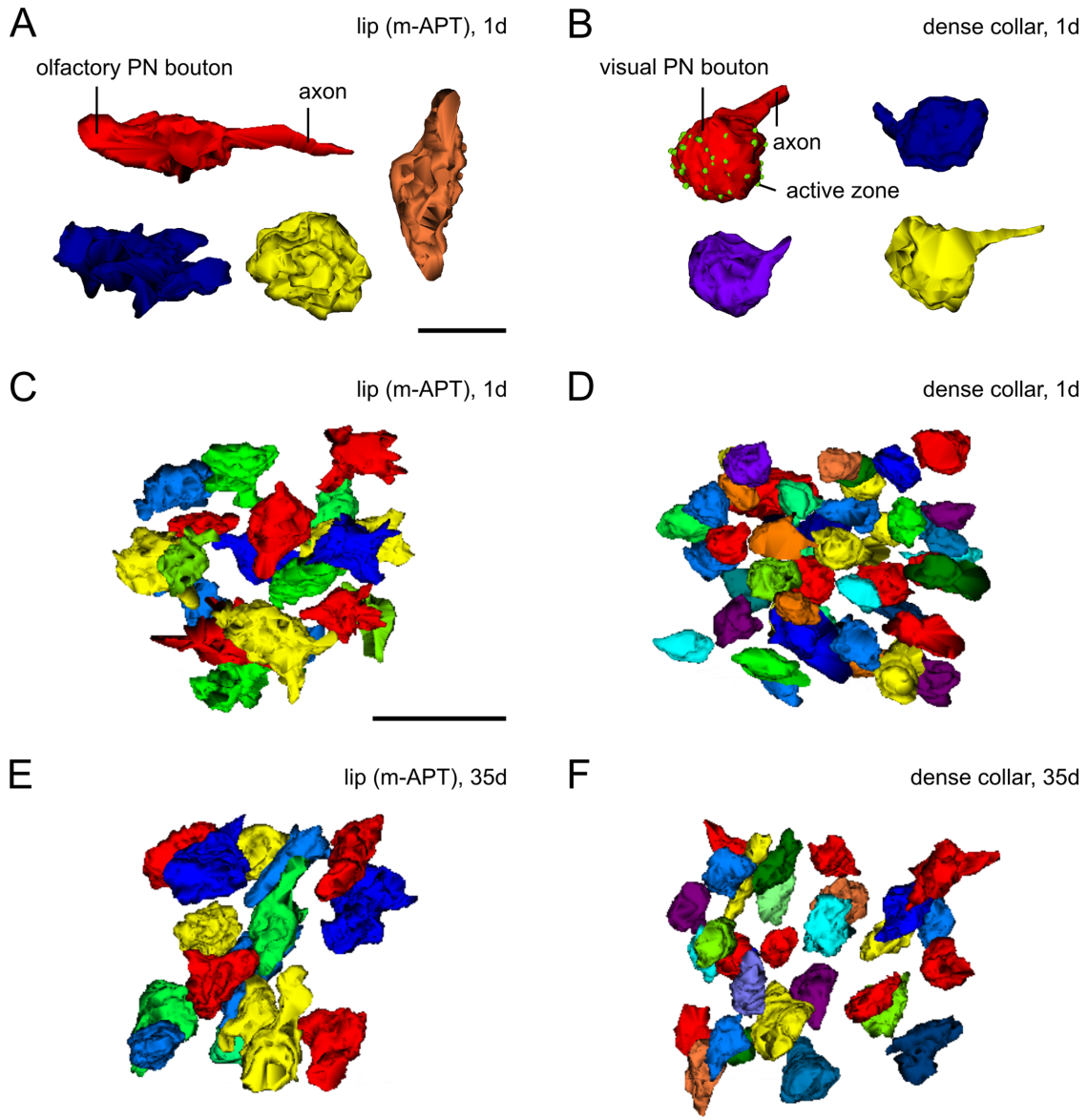

Figure 4. Shapes and packing densities of olfactory and visual projection neuron (PN) boutons in the calyx from ssEM reconstructions. **A,B:** Boutons are polymorphic in the calyx lip (reconstructed in A from the medial antennal-lobe protocerebral tract [m-APT] innervated lip of a 1-day-old bee) but unilobed in the dense region of the collar (B). Individual presynaptic sites are highlighted in green on the red bouton in (B). **C–F:** Compilation of reconstructed projection neuron boutons in a standard volume of 630 μm^3. The boutons are less densely packed in the lip of a 1-day-old worker (C) than in the dense collar (D). An age-related decrease in the packing density of boutons in the lip (C,E) and dense collar (D,F) is visible in these reconstructions. Scale bar = 2 μm in A (also applies to B); 5 μm in C (also applies to D–F).

volume in the old worker compared with the young worker (Mann–Whitney U-test: m-APT: 1 day–35 days, $P < 0.05$; l-APT: 1 day–35 days, $P < 0.001$; dense collar: 1 day–35 days, $P < 0.001$). Thus, overall, boutons were larger in olfactory areas of the calyx than in visual areas, and increased in size with the age of the bee. The olfactory boutons in the l-ATP innervated lip became larger with age than those in the m-ATP innervated lip.

In our serial sections, membranes of clear-core vesicles did not exhibit clear boundaries, making reliable quantification of individual vesicles impossible. However, projection neuron boutons have been reported to differ in cytoplasmic electron density, so as to constitute so-called light and dark boutons that most likely reflect differences in the abundance of small clear-core vesicles (Ganeshina and Menzel, 2001). Light (Fig. 3C) and dark boutons (Fig. 3D) were distinguished according to the gray scale value of their cytoplasm (light boutons: mean gray scale value 202 ± 17; dark boutons: mean gray scale value 163 ± 19; Wilcoxon test, $P < 0.05$). Both

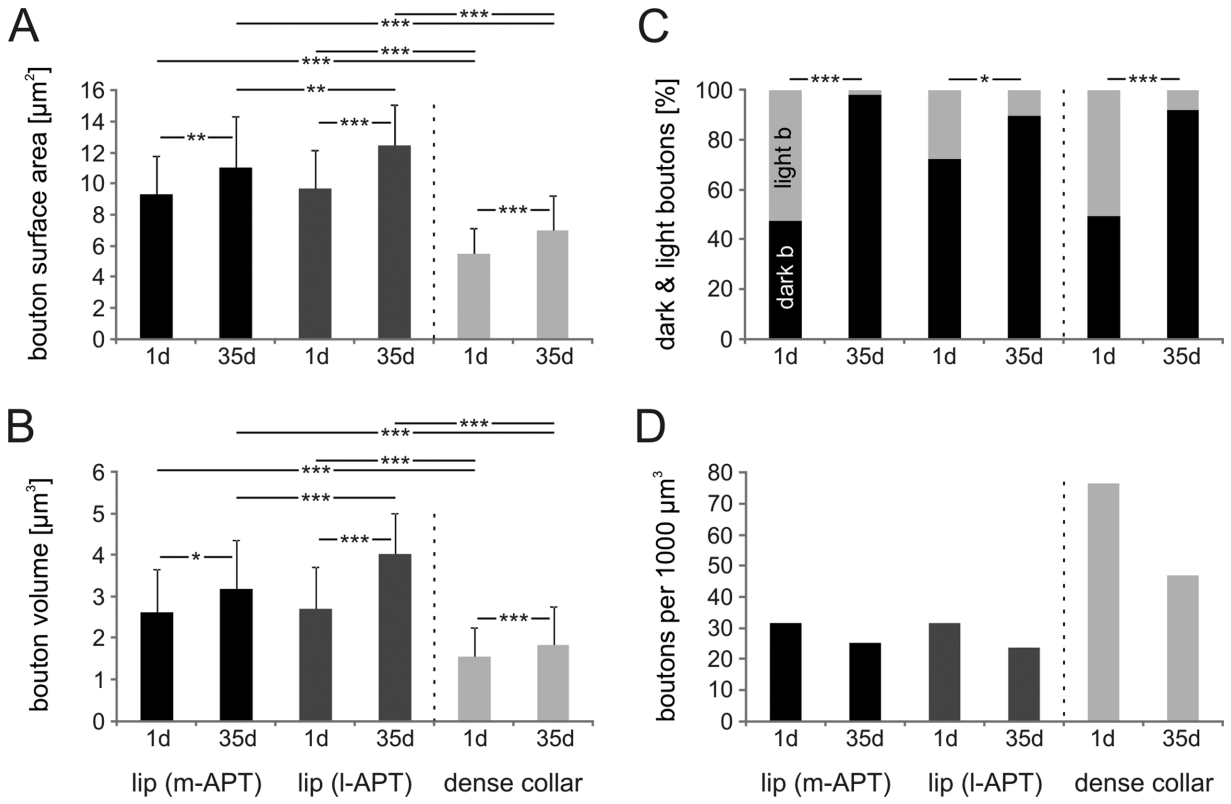

Figure 5. Age-related changes in size, subtype, and density of olfactory and visual projection neuron boutons revealed by ssEM. **A,B:** Age-related increase in bouton surface area and volume (mean ± SD). **C:** Percentage of light and dark projection neuron boutons. **D:** Packing density of reconstructed projection neuron boutons shows a decrease with age. The numbers of projection neuron boutons that could be reconstructed in their entirety were 40 (m-APT, 1 day), 56 (m-APT, 35 days), 36 (l-APT, 1 day), 57 (l-APT, 35 days), 89 (dense collar, 1 day), or 114 (dense collar, 35 days). The numbers of dark/light projection neuron boutons were 19/21 (m-APT, 1 day), 55/1 (m-APT, 35 days), 26/10 (l-APT, 1 day), 51/6 (l-APT, 35 days), 44/45 (dense collar, 1 day), and 105/9 (dense collar, 35 days). APT, antennal-lobe protocerebral tract; l, lateral; m, medial.

bouton phenotypes were interspersed within the neuropil and intermingled in no apparent pattern.

Contrary to an earlier report (Ganeshina and Menzel, 2001), these ultrastructural distinctions did not appear to correspond to bouton shape, and the size and number of mitochondria also did not differ between light and dark boutons. We observed changes in the percentage of light and dark boutons in the m-APT and l-APT innervated lip and the dense collar of bees between days 1 and 35 (Fig. 5C). Compared with a freshly emerged bee, the percentage of dark boutons was significantly more in a 35-day-old bee, whereas the reciprocal percentage of light boutons was significantly less (chi-square test: m-APT: 1 day–35 days, $\chi^2 = 33.97$, df $= 1$, $P < 0.001$; l-APT: 1 day–35 days, $\chi^2 = 4.61$; df $= 1$, $P < 0.05$; dense collar: 1 day–35 days, $\chi^2 = 46.60$, df $= 1$, $P < 0.001$).

Complete stacks of ssEM 3D reconstructions demonstrate that projection neuron boutons were less densely packed in the lip (illustrated by reconstructions from the m-APT innervated lip in Fig. 4C) than they were in the dense collar region (Fig. 4D) of a freshly emerged bee. The density of boutons in a defined volume of 1,000 µm^3 decreased with age in all three regions of interest between days 1 and 35 (Figs. 4E,F, 5D). This endorses the quantification of projection neuron bouton densities seen in synapsin-immunolabeled calyces, indicating that the boutons counted by light microscopy provide an accurate estimate of their packing density (Fig. 2A). However, the projection neuron bouton density quantified in 1,000 µm^3 from ssEM was lower than the density quantified in the same volume in synapsin-labeled whole-mount preparations, suggesting that boutons were identified by more scrupulous criteria from EM sections, and their numbers thus possibly underestimated.

Synaptic arrangement of projection neuron synapses in ssEM

Synaptic contacts were identified from their respective pre- and postsynaptic densities, and from the electron-dense staining of the presynaptic membrane at the so-called active zone (Fig. 3C–G), using criteria similar to

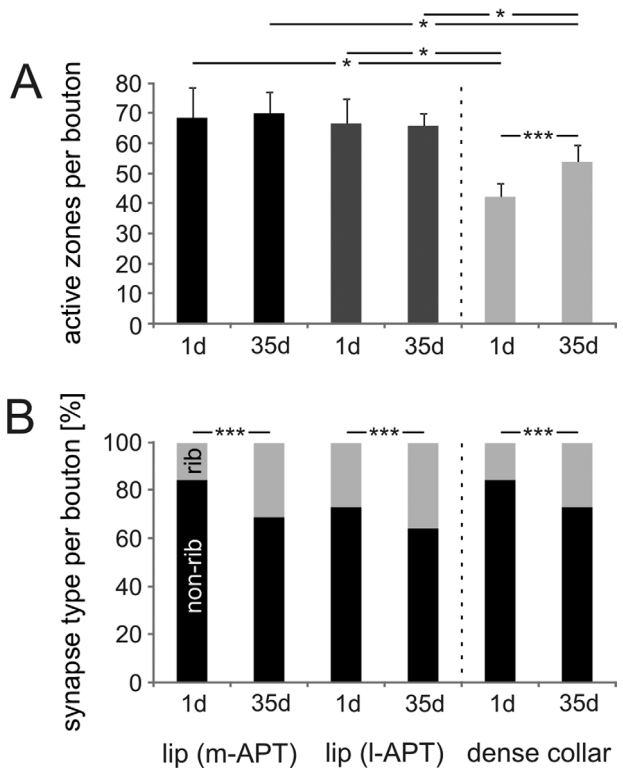

Figure 6. Number and organelle composition of olfactory and visual projection neuron bouton synapses. **A:** Number of presynaptic active zones per bouton (mean ± SD; $n = 10$). **B:** Percentage of non-ribbon and ribbon synapses per bouton. Corresponding numbers of non-ribbon/ribbon synapses: $n = 573/110$ (m-APT, 1 day); $n = 482/219$ (m-APT, 35 days); $n = 486/181$ (l-APT, 1 day); $n = 421/236$ (l-APT, 35 days); $n = 356/67$ (dense collar, 1 day); $n = 391/147$ (dense collar, 35 days). APT, antenal-lobe protocerebral tract; l, lateral; m, medial.

those adopted in previous studies (Ganeshina and Menzel, 2001; Yasuyama et al., 2002; Seid et al., 2005). The number of active zones per olfactory projection neuron bouton was about 30–60% more than per visual projection neuron bouton; this difference was seen in both a young 1-day-old worker bee (Fig. 6A; Wilcoxon test, Bonferroni corrected: m-APT–dense collar: $P < 0.017$; l-APT–dense collar, $P < 0.017$) and a 35-day-old forager (Wilcoxon test, Bonferroni corrected: m-APT–dense collar, $P < 0.017$; l-APT–dense collar, $P < 0.017$). In contrast, the number of active zones did not significantly differ between boutons in the m- and the l-APT innervated olfactory lip, for either the 1-day-old (Wilcoxon test, Bonferroni corrected: m-APT–l-APT, $P > 0.017$) or the 35-day-old bee (Wilcoxon test, Bonferroni corrected: m-APT–l-APT, $P > 0.017$). Whereas the total number of active zones per bouton showed an age-related increase in the dense region of the collar (Mann–Whitney U-test: dense collar: 1 day–35 days, $P < 0.001$), the total number of presynaptic sites in the m-APT and l-APT innervated lip regions did not significantly differ between the two ages (Mann–Whitney U-test: m-APT: 1 day–35 days, $P > 0.05$; l-APT: 1 day–35 days, $P > 0.05$). Overall, therefore, the synaptic organization of boutons from visual projection neurons showed clear quantitative differences from those of olfactory projection neurons, whereas the latter showed few differences between those of m-APT and those of l-APT origin.

In contact with their presynaptic membrane, active zones sometimes had a presynaptic density, which we will refer to as a ribbon, so-called for its resemblance to T-bar ribbons at fly synapses (Yasuyama et al., 2002; Butcher et al., 2012). We therefore classified synapses as either ribbon (those with a ribbon; Fig. 3F,G), or non-ribbon (those without; Fig. 3E). Presynaptic ribbons almost always exhibited a pedestal (Fig. 3F), but only rarely were these surmounted by a platform, so as to form the T-shape in cross section (Fig. 3G) typical of such structures in the projection neuron boutons of *Drosophila* (Yasuyama et al., 2002; Butcher et al., 2012). Ribbon and non-ribbon synapses were interspersed over the presynaptic membranes of both light and dark boutons. The proportions of the two types of synapses differed in the young and an old bee (Fig. 6B), with significantly more ribbon synapses in the older bee, and correspondingly significantly fewer non-ribbon synapses, differences that were found in all three calyx regions (χ^2 test: m-APT: 1 day–35 days, $\chi^2 = 43.74$, df $= 1$, $P < 0.001$; l-APT: 1 day–35 days, $\chi^2 = 11.84$, df $= 1$, $P < 0.001$; dense collar: 1 day–35 days, $\chi^2 = 18.04$, df $= 1$, $P < 0.001$).

Both ribbon and non-ribbon synapses formed by a single projection neuron bouton were usually approached by multiple postsynaptic elements (Fig. 3E–G). Membrane specializations were not obvious on these, however. Most postsynaptic profiles in contact with the active zone appeared in consecutive sections. They arose primarily from Kenyon cell dendrites identified from their slender dimensions, but infrequently also included larger profiles of extrinsic neurons (Ganeshina and Menzel, 2001; Yasuyama et al., 2002). The axons of projection neurons did not themselves form presynaptic sites (Fig. 4B), which thus formed only at the boutons, although the axons did receive occasional inputs from other cells, presumed to be extrinsic neurons. Synapses were most often arranged as dyads, triads, or tetrads in which one presynaptic element contacted two, three, or four postsynaptic profiles, respectively (Fig. 7). In the l-APT innervated lip region, ribbon and non-ribbon synapses formed significantly fewer dyads, but significantly more triads in the 35-day-old compared with the 1-day-old bee (Fig. 7B; Kruskal–Wallis H-test: monads: H $= 1.70$, df $= 1$, $P > 0.05$; dyads: H $= 10.11$, df $= 1$, $P < 0.01$; triads: H $= 8.94$, df $= 1$, $P < 0.01$; tetrads: H $= 1.70$, df $= 1$, $P > 0.05$; pentads: H $= 0.12$, df $= 1$, $P > 0.05$).

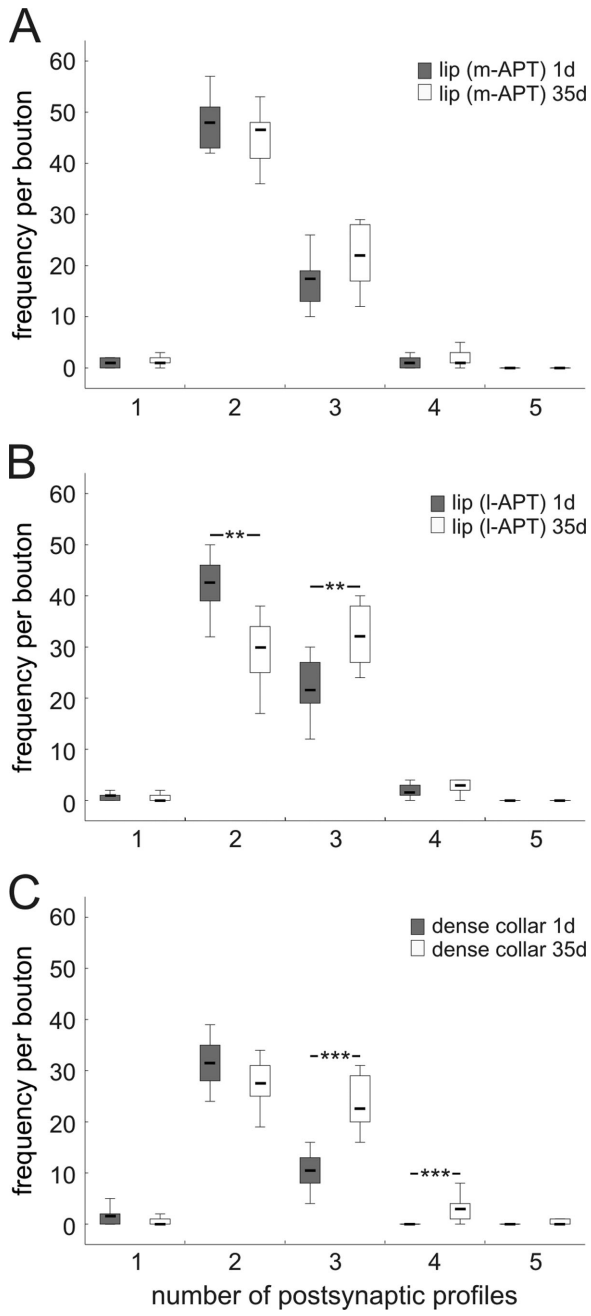

Figure 7. **A–C:** Numbers of postsynaptic profiles per active zone in the m-APT innervated lip (A), the l-APT innervated lip (B), and the dense collar (C) increase with age. Box plots represent the median and the 25% and 75% quartile numbers for the distribution of observed values. APT, antenal-lobe protocerebral tract; l, lateral; m, medial.

Similarly, synapses in the m-APT innervated lip region tended to form fewer dyads and more triads in the older forager than the 1-day-old bee (Fig. 7A; Kruskal–Wallis H-test: monads: $H = 0.27$, $df = 1$, $P > 0.05$; dyads: $H = 0.97$, $df = 1$, $P > 0.05$; triads: $H = 1.57$, $df = 1$, $P > 0.05$; tetrads: $H = 0.75$, $df = 1$, $P > 0.05$; pentads: $H = 0.0$, $df = 1$, $P > 0.05$). In the dense region of the collar, we found a significantly higher proportion of synapses that formed triads and tetrads in the forager compared with the 1-day-old bee (Fig. 7C; Kruskal–Wallis H-test: monads: $H = 2.07$, $df = 1$, $P > 0.05$; dyads: $H = 1.86$, $df = 1$, $P > 0.05$; triads: $H = 14.06$, $df = 1$, $P < 0.001$; tetrads: $H = 11.22$, $df = 1$, $P < 0.001$; pentads: $H = 1.19$, $df = 1$, $P > 0.05$). Thus, overall, synapses formed by the visual input boutons of the dense collar region increased with age in the forager (from about 95 to about 140), and all synapses, whether from visual or olfactory input bouton, had more ribbon synapses with age. In parallel, more postsynaptic elements accrued to each synapse, on average, in the forager bee than in the 1-day-old bee (Fig. 8).

DISCUSSION

This study provides the first detailed analysis of age-related changes of projection neuron boutons and the synaptic circuits to which they contribute in the olfactory lip and the visual collar of the mushroom body calyx in the adult honeybee. Our key findings indicate that during the behavioral transition from nursing to foraging projection neuron boutons exhibit an increase in their individual size, in the percentage of dark boutons, the number of ribbon synapses, and the average number of postsynaptic partners (Fig. 8). This refinement in synaptic connectivity is accompanied by a volume increase in the different calycal subdivisions and by a decrease in the packing density of synapsin-labeled boutons. The total number of synapsin-IR boutons both in the calyx lip and in the dense collar region reveals that the volume increase is not accompanied by the formation of new synapsin-labeled boutons. Collectively, these findings support the idea that the volume increase of the mushroom body calyx associated with age and/or experience is mainly caused by the outgrowth and connectivity of Kenyon cell dendrites. That outgrowth and its associated calycal synaptic changes could arise either from the increased age or from the foraging experience of 35-day-old honeybees relative to 1-day-old bees, and although our data do not allow us to distinguish in which combination these two factors may act, previous studies suggest that experience (Farris et al., 2001; Krofczik et al., 2008; Stieb et al., 2010, 2012) may play a significant role in such changes.

Our study addresses the synaptic features of the mushroom body calyx, which ssEM alone could provide. Alternative questions such as the number of boutons contributed by a projection neuron or the number of boutons contacted by a single Kenyon cell were not accessible to our methods, and must await the development of methods in honeybees that will enable the repeated study of single stained neurons.

A blend of ribbon and non-ribbon synapses characterizes both olfactory and visual projection neuron boutons

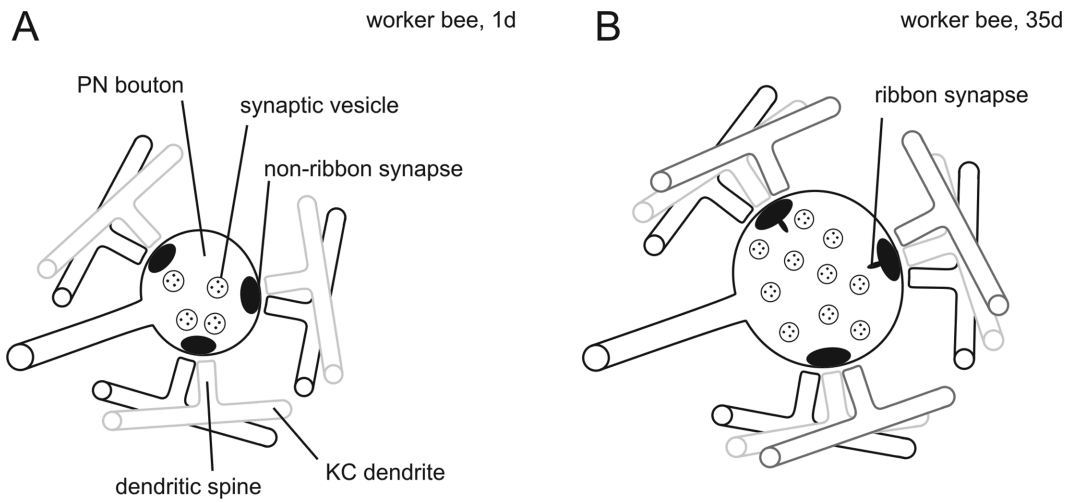

Figure 8. Diagram illustrating age-related synaptic rearrangement of projection neuron (PN) synapses in the calyx. **A:** In freshly emerged 1-day-old bees, mostly two postsynaptic elements, primarily tiny Kenyon cell dendritic spines, abut a single bouton release site. **B:** A month later, 35-day-old forager projection neuron boutons are larger and have more synaptic vesicles, more ribbon synapses, and a larger average number of postsynaptic partners. To effect these changes, the Kenyon cell (KC) dendrites undergo increased branching to form a dense network surrounding the bouton, thereby increasing the distance between individual boutons and the total volume of the calyx.

of the honeybee calyx although the exact mixture varies with age or experience. A blend of ribbon and non-ribbon synapses is also found in the fly's calyx (Butcher et al., 2012), and so may be general for this site. Likewise in the vertebrate retina, bipolar cells have synapses of both types, for example in the salamander and goldfish (Yang et al., 2003; Midorikawa et al., 2007). In the latter, ribbon synapses are associated with clusters of calcium channels, and calcium entering at the presynaptic site can diffuse to non-ribbon sites. Induction of presynaptic calcium current causes a transient rate of high-frequency vesicle fusion, followed by a delayed, sustained fusion outside the ribbon region (Midorikawa et al., 2007). It is possible that ribbon and non-ribbon synapses have a similar interplay in *Apis* projection neuron boutons. Thus, ribbon synapses could be readily activated in response to an olfactory or visual stimulus to provide strong, rapid transmission to Kenyon cells, and then a more sustained output from non-ribbon synapses only after these become facilitated by calcium entry from nearby ribbon synapses. Alternatively, a ribbon and non-ribbon synapse at a projection neuron terminal may be two different stages of the same synaptic site, non-ribbon synapses being simply ribbon synapses that have either lost their ribbon or have yet to assemble one. Thus non-ribbon synapses may adopt a nonfunctional state until they transform into ribbon synapses, or may play a different functional role in synaptic transmission, as in goldfish bipolar cells (Midorikawa et al., 2007). Either alternative would thus reflect an avenue for synaptic plasticity to transform the signaling of projection neurons depending on previous activity, in ways yet to be resolved.

Activity has previously been suggested to promote the formation of ribbon synapses. At crayfish neuromuscular junctions, for example, the recruitment of presynaptic dense bodies to existing synapses has been reported after long-term facilitation (Wojtowicz et al., 1994). Furthermore, synapses with depressed neurotransmitter release have recently been demonstrated after a molecular lesion in the T-bar ribbons caused by loss of *bruchpilot* (*brp*) function at *Drosophila* neuromuscular junctions (Hallermann et al., 2010). In contrast, in an apparently opposite finding, preventing projection neuron boutons in the fly's calyx from firing leads to an increase in the number of *brp* puncta, and possibly therefore of ribbon synapses (Kremer et al., 2010).

It is not clear how far the changes in ribbon synapse numbers that are evoked by changes in activity might predict the reciprocal changes in synaptic transmission at boutons having different numbers of ribbon synapses, such as we observe in young and experienced honeybees. In vertebrate photoreceptors the presynaptic ribbon is thought to funnel vesicles toward the presynaptic membrane (Parsons and Sterling, 2003), whereas in fly photoreceptors presynaptic T-bar ribbons support the high rates of tonic neurotransmitter release typical at the first synapse, as identified in *Drosophila* (Stuart et al., 2007). The increased numbers of ribbon synapses seen in olfactory and visual boutons during the behavioral transition from the 1-day-old bee to the forager may as a result reflect increased rates of neurotransmitter release at older boutons, and be associated with an increase in the number of postsynaptic partners.

It is also not clear how far in the honeybee calyx we can predict the outcome of synaptic plasticity seen in

flies or other species. Insect ribbon synapses exhibit a range of structures at their presynaptic densities, some also revealing specific differences.

So called T-bars, those with both a pedestal and platform, and thus T-shaped in cross section, are typical of synapses in higher Diptera (Zhai and Bellen, 2004), but not of ancestral forms (Shaw and Meinertzhagen, 1986). In flies, *brp* is a protein component of the platform but not the pedestal of the T-bar, both at larval neuromuscular junctions (Kittel et al., 2006; Fouquet et al., 2009) and at photoreceptor tetrad synapses (Hamanaka and Meinertzhagen, 2010). In locust photoreceptors, presynaptic densities lack a platform but nevertheless express immunoreactivity to *brp*, in that case at the tip of the pedestal (Leitinger et al., 2011), suggesting that the protein components of the presynaptic density may be similar in different insects, despite differences in their site of incorporation into synaptic organelles.

In order to evaluate differences in their synaptic populations, we need first to establish that light and dark projection neuron boutons are two true subpopulations revealed by differences in the density of their cytoplasm. Insect sensory neurons are sensitive to injury and undergo rapid degenerative changes that result in increased cytoplasmic electron density (Geisert and Altner, 1974; Brandstätter et al., 1991), raising the possibility that dark boutons in the calyx are simply light ones in the process of degenerating, a result, for example, of unintended damage during dissection.

Thus, fly photoreceptor terminals that undergo degeneration shrink, and have electron-dense cytoplasm, fewer synapses, and enlarged mitochondria (Brandstätter et al., 1991). For the olfactory system, antennal nerve crush in locusts procures reductions in antennal lobe volume that peak at about 3 days (Schürmann and Wechsler, 1970; Stern et al., 2012). Could the dark boutons of the honeybee calyx simply be light terminals undergoing degeneration? This seems unlikely. Not only did dark boutons have a similar volume and surface area and their synapses exhibit a similar size and density as those of light projection neuron boutons, but they were generally rather uniform in appearance. They thus lacked the variable stages that result from desynchronized degeneration seen in other sensory terminals (Brandstätter et al., 1991). Dark boutons are also described in previous work in the honeybee and in other species (bees: Ganeshina and Menzel, 2001; ants: Steiger, 1967; Seid and Wehner, 2008; flies: Butcher et al., 2012), and light and dark boutons have been speculated to reflect different functional states of a single class of a projection neuron terminal (Steiger, 1967).

Both light and dark projection neuron boutons contain occasional profiles of dense-core vesicles. Because each projection neuron axon forms multiple collaterals in the calyx, we might expect that all the boutons of a single axon should either have, or lack, dense-core vesicles. However such vesicles may in fact be directed to selected boutons, possibly depending on the local activity of its targets, and the vesicles may not always be sampled in different boutons of the same axon in the same sections. Classically associated with the packaging and release of neuropeptides and some aminergic transmitters (De Camilli and Jahn, 1990; Bauerfeind and Huttner, 1993; Kelly, 1993), dense-core vesicles are predicted to release their contents away from synapses (De Camilli and Jahn, 1990) and to act at distant sites, where some may modulate synaptic transmission (Marder and Thirumalai, 2002). They are predicted to exert neuromodulatory effects on the processing of olfactory and visual signals either within or between microglomeruli, but analysis of this possibility must first await identification of the dense-core vesicles' contents. Neuropeptide signaling in particular is functionally very diverse (Nässel, 2009) and even though at least 40 *Drosophila* genes encode neuropeptide receptors (Hewes and Taghert, 2001), very few neuropeptides have been mapped in detail in the adult central nervous system (Nässel and Winther, 2011). The dense-core vesicles may also contain biogenic amines, and because octopamine, dopamine, and serotonin, in addition to the neuropeptide FMRFamide, have been identified in the calyces of the honeybee (Schürmann et al., 1989; Kreissel et al., 1994; Blenau et al., 1999), sparse boutons that contain dense-core vesicles may belong to aminergic extrinsic neurons as well as projection neurons. Further studies are obviously needed to identify extrinsic mushroom body neurons and their vesicle cargos in greater detail.

As at multiple-contact synapses in the fly's brain (Prokop and Meinertzhagen, 2006), multiple postsynaptic partners contact the same presynaptic site, in an arrangement seen at both olfactory and visual projection neuron boutons of the honeybee calyx. Kenyon cell dendritic spines contribute most of these postsynaptic elements, with occasional contributions from extrinsic neurons (Schürmann, 1982; Ganeshina and Menzel, 2001; Yasuyama et al., 2002; Butcher et al., 2012). In *Drosophila*, the dendrites of all three classes of Kenyon cell appear to arborize more or less broadly in the mushroom body calyx, and individual projection neurons contact multiple classes of Kenyon cells (Tanaka et al., 2008; Leiss et al., 2009). Similarly, in the honeybee the spiny class I Kenyon cells in particular have wide-field dendritic arbors (Strausfeld, 2002).

The number of postsynaptic partners contacting a single presynaptic site varies considerably, ranging from one to five, but typical synapses are dyads in a 1-day-old bee and dyads or triads in the forager. Similarly, in the ant

Cataglyphis albicans, forager synapses are most often triads, with a maximum of six postsynaptic partners (Seid and Wehner, 2008). The outcome of these changes in Hymenoptera is that, because neurogenesis is absent in the adult honeybee brain (Fahrbach et al., 1995) and Kenyon cell number remains constant with age in ants (Gronenberg et al., 1996), more contacts to dendrites can be established. These changes are probably achieved mainly by the outgrowth and extension of Kenyon cell dendrites in foragers (Farris et al., 2001). Given that we find that boutons are lost during the transition from nursing to foraging, some Kenyon cell postsynaptic elements must therefore switch to the surviving boutons, thus selectively concentrating the inputs of the latter. Our numerical analyses in the visual collar indicate that each presynaptic projection neuron bouton in the 1-day-old bee must diverge to provide input upon about 95 Kenyon cell dendritic profiles, whereas in the forager this number is about 140, an increased ratio of about 1.5:1. In the lip this effect is less pronounced but appears more obvious in the l-APT subregion.

As a result, we infer that Kenyon cell dendritic spines are the key to the reorganization of microglomeruli that occurs during the transition between nurse and forager. That reorganization accompanies an age-dependent division of labor that must also incur altered patterns of visual and olfactory neuronal activity. Thus dendritic spines should be the focus of further investigations in honeybee Kenyon cells, and elsewhere indeed are suggested to play a crucial role in forming the microcircuits responsible for learning and memory (Yuste and Bonhöffer, 2001). Reflecting this direction, a recent study in the honeybee has shown that calcium-mediated kinase II (CaMKII), a protein known to be associated with synaptic plasticity, is highly enriched in class I Kenyon cell dendritic spines (Pasch et al., 2011), and microglomeruli become reorganized after formation of stable olfactory long-term memory (Hourcade et al., 2010).

In addition to their Kenyon cell targets, projection neuron boutons themselves also exhibit morphological changes during the transition from nursing to foraging. The surface area and volume of boutons increases in both the lip and the dense region of the collar, along with a reduction in bouton number. Volume increases in boutons of the honeybee lip together with a decrease in bouton number have previously been proposed based on increases in anti-synapsin immunoreactivity (Krofczik et al., 2008), and although alternative explanations might have been possible, our EM data now validate this suggestion. Two species of ants with an age-dependent division of labor comparable to honeybee workers also reveal similar changes. The volume of boutons is enlarged in older and more experienced workers compared with young workers (*Pheidole dentata*: Seid et al., 2005; *Cataglyphis albicans*: Seid and Wehner, 2009). In *Drosophila*, size changes in boutons are dependent on neuronal activity (Kremer et al., 2010), and our data are consistent with this possibility for honeybee projection neurons also. In addition, our study reveals that boutons relaying different sensory information are not the same, those innervating the lip of both 1-day-old bees and old foragers having larger boutons and more presynaptic sites than those in the dense region of the collar.

Based on similar observations in *Cataglyphis*, Seid and Wehner (2009) suggest that olfactory inputs signaled by projection neuron boutons in the lip are stronger and more likely to propagate in the calyx than visual signals because higher synapse numbers and thus elevated synaptic efficacy have been implicated in enhanced olfactory perception (Acebes and Ferrus, 2001). In addition, the number of presynaptic release sites per visual projection neuron bouton is larger in the forager than in the 1-day-old bee, compatible with a strengthening in the signals transmitted to postsynaptic elements when the worker honeybee leaves the dark hive to forage, and imposes increased patterns of stimulation on the visual system.

Several studies report an increase in mushroom body volume with behavioral experience during the transition from nursing to foraging (bees: Withers et al., 1993; Durst et al., 1994; ants: Gronenberg et al., 1996; Kühn-Bühlmann and Wehner, 2006). By using synapsin immunolabeling of whole-mount brains we show here that the increased volume of calycal subdivisions seen in honeybee foragers is accompanied by a decrease in the packing density of synapsin-immunolabeled boutons, and increased spacing between individual boutons. Given our estimates that no new synapsin-labeled boutons form in the calyx of foragers, the increased size of boutons during the behavioral transition cannot provide a satisfactory explanation for the volume increase of the forager's calyx. As previously concluded by Farris et al. (2001), we infer instead that an outgrowth of Kenyon cell dendrites and an extension of Kenyon cell arbors are the main structural components of the calycal volume increase. A similar conclusion has been reached based on tubulin immunolabeling of Kenyon cell primary branches in callows and foragers of the ant *Cataglyphis fortis* (Stieb et al., 2010). The lower density of presynaptic boutons in the forager calyx must be offset by the additional space occupied by the outgrowth of Kenyon cell dendrites. However, it is not clear whether the increased arborization of Kenyon cell dendrites (Farris et al., 2001) displaces the packing of presynaptic boutons to ensure their wider spacing, and the chronological order of these events still needs to be elucidated.

Our findings have used ssEM to investigate the synaptic organization of projection neuron boutons, and are a

TABLE 3.

Estimates of Calycal Synaptic Connections in *Drosophila* and *Apis*[1]

Olfactory PN bouton characteristics	Female fly (4-days-old)	Worker bee (1-day-old)	Worker bee (35-days-old)
AZ per bouton	40*	67	68
AZ packing density per bouton surface area	2*	7	6
Volumetric density of AZ per μm^3 in the calyx (fly)/in the lip (bee)	3*	2	2
Boutons per calyx (fly)/per lip (bee)	1,115**	177,126	157,773
AZ per calyx (fly)/per lip (bee)	44,600*	11,867,442	10,728,564
Postsynaptic partners per AZ	6*	2	3
Postsynaptic partners per calyx (fly)/per lip (bee)	267,600*	23,734,884	32,185,692

[1]Values and extrapolated mean numbers are given per total calyx volume in the fly and per calyx lip volume in the bee. Findings in the fly's calyx derive from *Butcher et al. (2012) and **Turner et al. (2008). AZ, active zone; PN, projection neuron.

first step in analyzing the circuits of the calyx, and subsequently a means to understand the neuronal basis of honeybee behavioral transitions. Comparing our findings with those from the calyx of *Drosophila* (Butcher et al., 2012), which mainly receives olfactory input from the antennal lobe, reveals interesting similarities but also clear differences (Table 3). The most evident difference is the dense enrichment of olfactory synaptic circuits in the lip of the honeybee calyx. Olfactory boutons in the calyx of a young bee form on average 70 active zones compared with about 40 in the fly. In the fly, an estimated 1,115 projection neuron boutons (Turner et al., 2008) form roughly 44,600 active zones per calyx. In the young bee, we estimate more than 177,000 boutons and around 12 million active zones per calyx lip. Synaptic divergence appears higher in the fly, on the other hand, with 6 postsynaptic elements on average per release site, but up to 14 elements. However, the innervation ratio of projection neuron boutons to postsynaptic elements is around 100 times higher in the bee compared with the fly and even increases in the forager bee. The obvious expansion of synaptic modules in the calyx in the honeybee, and other Hymenoptera (Groh and Rössler, 2011), is most likely related to the enormous role played by olfaction throughout the adult life of a bee.

Recent studies on both the honeybee and *Cataglyphis* ants show that these synaptic microcircuits are affected by brood care (Groh et al., 2004, 2006), sensory experience (Stieb et al., 2010, 2012), and the formation of stable long-term memories (Hourcade et al., 2010). This susceptibility immediately suggests an active role played by the calycal microcircuits of the mushroom body in lifelong plasticity and the adjustments to neuronal circuits underlying behavioral plasticity in a social insect.

ACKNOWLEDGMENTS

We thank Dirk Ahrens for bee-keeping expertise, Erich Buchner for the kind gift of anti-synapsin antibodies, Kornelia Grübel for expert technical assistance and help with data evaluation, Lena Schumacher for aligning electron micrograph image stacks, and, for their introductions to software, Nancy Butcher (Reconstruct) and Christina Kelber (AMIRA).

LITERATURE CITED

Abel R, Rybak J, Menzel R. 2001. Structure and response patterns of olfactory interneurons in the honeybee, *Apis mellifera*. J Comp Neurol 437:363–383.

Acebes A, Ferrus A. 2001. Increasing the number of synapses modifies olfactory perception. J Neurosci 21:6264–6273.

Bailey CH, Kandel ER. 1993. Structural changes accompanying memory storage. Annu Rev Physiol 55:397–426.

Bauerfeind R, Huttner WB. 1993. Biogenesis of constitutive secretory vesicles, secretory granules and synaptic vesicles. Curr Opin Cell Biol 5:628–635.

Blenau W, Schmidt M, Faensen D, Schürmann FW. 1999. Neurons with dopamine-like immunoreactivity target mushroom body Kenyon cell somata in the brain of some hymenopteran insects. Int J Insect Morphol 28:203–210.

Brandstätter J, Shaw SR, Meinertzhagen IA. 1991. Terminal degeneration and synaptic disassembly following receptor photoablation in the retina of the fly's compound eye. J Neurosci 11:1930–1941.

Brandt R, Rohlfing T, Rybak J, Krofczik S, Maye A, Westerhoff M, Hege HC, Menzel R. 2005. Three-dimensional average-shape atlas of the honeybee brain and its applications. J Comp Neurol 492:1–19.

Butcher NJ, Friedrich AB, Lu Z, Tanimoto H, Meinertzhagen IA. 2012. Different classes of input and output neurons reveal new features in microglomeruli of the adult *Drosophila* mushroom body calyx. J Comp Neurol 520:2185–2201.

Davis RL. 2005. Olfactory memory formation in *Drosophila*: from molecular to systems neuroscience. Annu Rev Neurosci 28:275–302.

De Camilli P, Jahn R. 1990. Pathways to regulated exocytosis in neurons. Annu Rev Physiol 52:625–645.

Durst C, Eichmüller S, Menzel R. 1994. Development and experience lead to increased volume of subcompartments of the honeybee mushroom body. Behav Neural Biol 62: 259–263.

Ehmer B, Gronenberg W. 2002. Segregation of visual input to the mushroom bodies in the honeybee (*Apis mellifera*). J Comp Neurol 451:362–373.

Ehmer B, Reeve HK, Hoy RR. 2001. Comparison of brain volumes between single and multiple foundresses in the paper wasp *Polistes dominulus*. Brain Behav Evol 57:16–168.

Fahrbach SE. 2006. Structure of the mushroom bodies of the insect brain. Annu Rev Entomol 51:209–232.

Fahrbach SE, Strande JL, Robinson GE. 1995. Neurogenesis is absent in the brains of adult honey bees and does not explain behavioral neuroplasticity. Neurosci Lett 197: 145–148.

Fahrbach SE, Moore D, Capaldi EA, Farris SM, Robinson GE. 1998. Experience-expectant plasticity in the mushroom bodies in the honey bee *Apis mellifera*. Learn Mem 5:115–123.

Farris SM, Robinson GE, Davis RL, Fahrbach SE. 1999. Larval and pupal development of the mushroom bodies in the honey bee, *Apis mellifera*. J Comp Neurol 414:97–113.

Farris SM, Robinson, GE, Fahrbach SE. 2001. Experience- and age-related outgrowth of intrinsic neurons in the mushroom bodies of the adult worker honeybee. J Neurosci 21: 6395–6404.

Fiala JC. 2005. Reconstruct: a free editor for serial section microscopy. J Microsc 218:52–61.

Fiala JC, Harris KM. 2001. Extending unbiased stereology of brain ultrastructure to three-dimensional volumes. J Am Med Inform Assoc 8:1–16.

Fouquet W, Owald D, Wichmann C, Mertel S, Depner H, Dyba M, Hallermann S, Kittel, R, Eimer S, Sigrist SJ. 2009. Maturation of active zone assembly by *Drosophila* Bruchpilot. J Cell Biol 186:129–145.

Frambach I, Rössler W, Winkler M, Schürmann F. 2004. F-actin at identified synapses in the mushroom body neuropil of the insect brain. J Comp Neurol 475:303–314.

Galizia CG, Rössler W. 2010. Parallel olfactory systems in insects: anatomy and function. Annu Rev Entomol 55: 399–420.

Ganeshina O, Menzel R. 2001. GABA-immunoreactive neurons in the mushroom bodies of the honeybee: an electron microscopic study. J Comp Neurol 437:335–349.

Geisert B, Altner H. 1974. Analysis of the sensory projection from the tarsal sensilla of the blow-fly (*Phormia terraenovae* Rob.-Desv., Diptera). Cell Tissue Res 150:249–259.

Gerber B, Tanimoto H, Heisenberg M. 2004. An engram found? Evaluating the evidence from fruit flies. Curr Opin Neurobiol 14:737–744.

Giurfa M. 2007. Behavioral and neural analysis of associative learning in the honeybee: a taste from the magic well. J Comp Physiol A 193:801–824.

Godenschwege TA, Reisch D, Diegelmann S, Eberle K, Funk N, Heisenberg M, Hoppe V, Hoppe J, Klagges BRE, Martin JR, Nikitina E, Putz G, Reifegertse R, Reisch N, Rister J, Schaupp M, Scholz H, Schwärzel M, Werner U, Zars TD, Buchner S, Buchner E. 2004. Flies lacking all synapsins are unexpectedly healthy but are impaired in complex behaviour. Eur J Neurosci 20:611–622.

Groh C, Rössler W. 2011. Comparison of microglomerular structures in the mushroom body calyx of neopteran insects. Arthropod Struct Dev 40:358–367.

Groh C, Tautz J, Rössler W. 2004. Synaptic organization in the adult honey bee brain is influenced by brood-temperature control during pupal development. Proc Natl Acad Sci U S A 101:4268–4273.

Groh C, Ahrens D, Rössler W. 2006. Environment- and age-dependent plasticity of synaptic complexes in the mushroom bodies of honeybee queens. Brain Behav Evol 68:1–14.

Gronenberg W. 2001. Subdivisions of hymenopteran mushroom body calyces by their afferent supply. J Comp Neurol 436:474–489.

Gronenberg W, Heeren S, Hölldobler B. 1996. Age-dependent and task-related morphological changes in the brain and the mushroom bodies of the ant *Camponotus floridanus*. J Exp Biol 199:2011–2019.

Grünewald B. 1999. Morphology of feedback neurons in the mushroom body of the honeybee, *Apis mellifera*. J Comp Neurol 404:114–126.

Hallermann S, Kittel R, Wichmann C, Weyhersmüller A, Fouquet W, Mertel S, Owald D, Eimer S, Depner H, Schwärzel M, Sigrist SJ, Heckmann M. 2010. Naked dense bodies provoke depression. J Neurosci 30:14340–14345.

Hamanaka Y, Meinertzhagen IA. 2010. Immunocytochemical localization of synaptic proteins to photoreceptor synapses of *Drosophila melanogaster*. J Comp Neurol 518: 1133–1155.

Hammer M. 1993. An identified neuron mediates the unconditioned stimulus in associative olfactory learning in honeybees. Nature 366:59–63.

Heisenberg M. 2003. Mushroom body memoir: from maps to models. Nat Rev Neurosci 4:266–275.

Hewes RS, Taghert PH. 2001. Neuropeptides and neuropeptide receptors in the *Drosophila melanogaster* genome. Genome Res 11:1126–1142.

Hofbauer A, Ebel T, Waltenspiel B, Oswald P, Chen YC, Halder P, Biskup S, Lewandrowski U, Winkler C, Sickmann A, Buchner S, Buchner E. 2009. The Wuerzburg hybridoma library against *Drosophila* brain. J Neurogenet 23:78–91.

Hourcade B, Muenz TS, Sandoz JC, Rössler W, Devaud JM. 2010. Long-term memory leads to synaptic reorganization in the mushroom bodies: a memory trace in the insect brain? J Neurosci 30:6461–6465.

Hoyer S, Liebig J, Rössler W. 2005. Biogenic amines in the ponerine ant *Harpegnathos saltator*: serotonin and dopamine immunoreactivity in the brain. Arthropod Struct Dev 34:429–440.

Ismail N, Robinson GE, Fahrbach SE. 2006. Stimulation of muscarinic receptors mimics experience-dependent plasticity in the honey bee brain. Proc Natl Acad Sci U S A 103:207–211.

Kelly RB. 1993. Storage and release of neurotransmitters. Cell 72(suppl):43–53.

Kirschner S, Kleineidam CJ, Zube C, Rybak J, Grünewald B, Rössler W. 2006. Dual olfactory pathway in the honeybee, *Apis mellifera*. J Comp Neurol 499:933–952.

Kittel R, Wichmann C, Rasse T, Fouquet W, Schmidt M, Schmid A, Wagh DA, Pawlu C, Kellner RR, Willig KI, Hell SW, Buchner E, Heckmann M, Sigrist SJ. 2006. Bruchpilot promotes active zone assembly, Ca^{2+} channel clustering, and vesicle release. Science 312:1051–1054.

Klagges BRE, Heimbeck G, Godenschwege TA, Hofbauer A, Pflugfelder GO, Reifegerste R, Reisch D, Schaupp M, Buchner S, Buchner E. 1996. Invertebrate synapsins: a single gene codes for several isoforms in *Drosophila*. J Neurosci 16:3154–3165.

Kolb B, Wishaw IQ. 1998. Brain plasticity and behavior. Annu Rev Psychol 49:43–64.

Kreissel S, Eichmüller S, Bicker G, Rapus J, Eckert M. 1994. Octopamine-like immunoreactivity in the brain and subesophageal ganglion of the honeybee. J Comp Neurol 348: 583–595.

Kremer M, Christiansen F, Leiss F, Paehler M, Knapek S, Andlauer TFM, Förstner F, Kloppenburg P, Sigrist SJ, Tavosanis G. 2010. Structural long-term changes at mushroom body input synapses. Curr Biol 20:1938–1944.

Krofczik S, Khojasteh U, de Ibarra NH, Menzel R. 2008. Adaptation of microglomerular complexes in the honeybee mushroom body lip to manipulations of behavioral maturation and sensory experience. Dev Neurobiol 68:1007–1017.

Kühn-Bühlmann S, Wehner R. 2006. Age-dependent and task-related volume changes in the mushroom bodies of visually guided desert ants, *Cataglyphis bicolor*. J Neurobiol 66: 511–521.

Leiss F, Groh C, Butcher NJ, Meinertzhagen IA, Tavosanis G. 2009. Synaptic organization in the adult *Drosophila* mushroom body calyx. J Comp Neurol 517:808–824.

Leitinger G, Masich S, Neumüller J, Pabst MA, Pavelka M, Rind FC, Shupliakov O, Simmons PJ, Kolb D. 2011. Structural organization of the presynaptic density at identified synapses in the locust central nervous system. J Comp Neurol 400:384–400.

Marder E, Thirumalai V. 2002. Cellular, synaptic and network effects of neuromodulation. Neural Netw 15:479–93.

Meinertzhagen IA. 1996. Ultrastructure and quantification of synapses in the insect nervous system. J Neurosci Methods 69:59–73.

Meinertzhagen IA. 2001. Plasticity in the insect nervous system. Adv Insect Physiol 28:84–167.

Menzel R, Giurfa M. 2001. Cognitive architecture of a minibrain: the honeybee. Trends Cogn Sci 5:62–71.

Midorikawa M, Tsukamoto Y, Berglund K, Ishii M, Tachibana M. 2007. Different roles of ribbon-associated and ribbon-free active zones in retina bipolar cells. Nat Neurosci 10: 1268–1276.

Mobbs PG. 1982. The brain of the honeybee *Apis mellifera* 1. The connections and spatial organization of the mushroom bodies. Philos Trans R Soc B 298:309–354.

Nässel DR. 2009. Neuropeptide signaling near and far: how localized and timed is the action of neuropeptides in brain circuits? Invertebr Neurosci 9:57–75.

Nässel DR, Winther AME. 2010. *Drosophila* neuropeptides in regulation of physiology and behavior. Progr Neurobiol 92: 42–104.

O'Donnell S, Donlan NA, Jones TA. 2004. Mushroom body structural change is associated with division of labor in eusocial wasp workers (*Polybia aequatorialis*, Hymenoptera: Vespidae). Neurosci Lett 356:159–162.

Parsons T, Sterling P. 2003. Synaptic ribbon. Conveyer belt or safety belt. Neuron 37:379–382.

Pasch E, Muenz TS, Rössler W. 2011. CaMKII is differentially localized in synaptic regions of Kenyon cells within the mushroom bodies of the honeybee brain. J Comp Neurol 519:3700–3712.

Paulk AC, Phillips-Portillo J, Dacks AM, Fellous J, Gronenberg W. 2008. The processing of color, motion, and stimulus timing are anatomically segregated in the bumblebee brain. J Neurosci 28:6319–6332.

Prokop A, Meinertzhagen IA. 2006. Development and structure of synaptic contacts in *Drosophila*. Semin Cell Dev Biol 17:20–30.

Rössler W, Groh C. 2012. Plasticity of synaptic microcircuits in the mushroom-body calyx of the honey bee. In: Galizia CG, Eisenhardt D, Giurfa M, editors. Honeybee neurobiology and behavior. Berlin: Springer Verlag. p 141–151.

Rybak J, Menzel R. 1993. Anatomy of the mushroom bodies in honey bee brain: the neuronal connections of the alpha-lobe. J Comp Neurol 334:444–465.

Schürmann FW. 1982. On synaptic connexions, tracts, and compartments in the brain of the honeybee. In: Breed MD, Michener CD, Evans HE, editors. The biology of social insects. Boulder, CO: Westview Press. p 390–394.

Schürmann FW, Wechsler W. 1970. Synapsen im Antennhügel von *Locusta migratoria*. Z Zellforsch Mikrosc Anat 95: 223–248.

Schürmann FW, Elekes K, Geffard M. 1989. Dopamine-like immunoreactivity in the bee brain. Cell Tissue Res 256: 43–58.

Seid MA, Wehner R. 2008. Ultrastructure and synaptic differences of the boutons of the projection neurons between the lip and collar regions of the mushroom bodies in the ant, *Cataglyphis albicans*. J Comp Neurol 507:1102–1108.

Seid MA, Wehner R. 2009. Delayed axonal pruning in the ant brain: a study of developmental trajectories. Dev Neurobiol 69:350–364.

Seid M, Harris KM, Traniello JF. 2005. Age-related changes in the number and structure of synapses in the lip region of the mushroom bodies in the ant *Pheidole dentata*. J Comp Neurol 488:269–277.

Shaw SR, Meinertzhagen IA. 1986. Evolution of synaptic connections among homologous neurons. Proc Natl Acad Sci U S A 83:7961–7965.

Sinakevitch I, Strausfeld NJ. 2006. Comparison of octopamine-like immunoreactivity in the brains of the fruit fly and blow fly. J Comp Neurol 494:460–475.

Steiger U. 1967. Über den Feinbau des Neuropils im Corpus pedunculatum der Waldameise. Z Zellforsch 81:511–536.

Stern M, Scheiblich H, Eickhoff R, Didwischus N, Bicker G. 2012. Regeneration of olfactory afferent axons in the locust. J Comp Neurol 520:679–693.

Stieb SM, Muenz TS, Wehner R, Rössler W. 2010. Visual experience and age affect synaptic organization in the mushroom bodies of the desert ant *Cataglyphis fortis*. Dev Neurobiol 70:408–423.

Stieb SM, Hellwig A, Wehner R, Rössler W. 2012. Visual experience affects both behavioral and neuronal aspects in the individual life history of the desert ant *Cataglyphis fortis*. Dev Neurobiol 72:729–742.

Strausfeld NJ. 2002. Organization of the honey bee mushroom body: representation of the calyx within the vertical and gamma lobes. J Comp Neurol 450:4–33.

Stuart AE, Borycz J, Meinertzhagen IA. 2007. The dynamics of signaling at the histaminergic photoreceptor synapse of arthropods. Prog Neurobiol 82:202–227.

Tanaka NK, Tanimoto H, Ito K. 2008. Neuronal assemblies of the *Drosophila* mushroom body. J Comp Neurol 508:711–755.

Technau GM. 1984. Fiber number in the mushroom bodies of adult *Drosophila melanogaster* depends on age, sex and experience. J Neurogenet 1:113–126.

Trujillo-Cenóz O, Melamed J. 1962. Electron microscope observations on the calyces of the insect brain. J Ultrastruct Res 7:389–398.

Turner GC, Bazhenov M, Laurent G. 2008. Olfactory representations by Drosophila mushroom body neurons. J Neurophysiol 99:734–746.

Withers GS, Fahrbach SE, Robinson GE. 1993. Selective neuroanatomical plasticity and division of labour in the honeybee. Nature 364:238–240.

Wojitowicz J, Marin L, Atwood H. 1994. Activity-induced changes in synaptic release sites at the crayfish neuromuscular junction. J Neurosci 14:3688–3703.

Yang C, Zhang J, Yazulla S. 2003. Differential synaptic organization of GABAergic bipolar cells and non-GABAergic (glutamatergic) bipolar cells in the tiger salamander retina. J Comp Neurol 455:187–197.

Yasuyama K, Meinertzhagen IA, Schürmann F. 2002. Synaptic organization of the mushroom body calyx in *Drosophila melanogaster*. J Comp Neurol 445:211–226.

Yuste R, Bonhoeffer T. 2001. Morphological changes in dendritic spines associated with long-term synaptic plasticity. Annu Rev Neurosci 24:1071–1089.

Zhai R, Bellen H. 2004. The architecture of the active zone in the presynaptic nerve terminal. Physiology (Bethesda) 19:262–270.

Zube C, Rössler W. 2008. Caste- and sex-specific adaptations within the olfactory pathway in the brain of the ant *Camponotus floridanus*. Arthropod Struct Dev 37:469–479.

Zube C, Kleineidam CJ, Kirschner S, Neef J, Rössler W. 2008. Organization of the olfactory pathway and odor processing in the antennal lobe of the ant *Camponotus floridanus*. J Comp Neurol 506:425–441.